SRI International

Final Report • January 1992

EXCITED NEGATIVE IONS AND MOLECULES AND NEGATIVE ION PRODUCTION

James R. Peterson, Senior Staff Scientist
Molecular Physics Laboratory

Contract No. F49620-89-K-0002
SRI Project No. PHY-6952
MP 91-275

Prepared for:

Air Force Office of Scientific Research
Building 410
Bolling Air Force Base
Washington, DC 20332-6448

Attention: Lt. Col. James A. Lupo

Approved:

Donald J. Eckstrom, Director
Molecular Physics Laboratory

David M. Golden
Vice President
Physical Sciences Division

Final Report • January 1992

EXCITED NEGATIVE IONS AND MOLECULES AND NEGATIVE ION PRODUCTION

James R. Peterson, Senior Staff Scientist
Molecular Physics Laboratory

Contract No. F49620-89-K-0002
SRI Project No. PHY-6952
MP 91-275

Prepared for:

Air Force Office of Scientific Research
Building 410
Bolling Air Force Base
Washington, DC 20332-6448

Attention: Lt. Col. James A. Lupo

Approved:

Donald J. Eckstrom, Director
Molecular Physics Laboratory

David M. Golden
Vice President
Physical Sciences Division

SRI International 333 Ravenswood Avenue • Menlo Park, CA 94025-3493 • (415) 326-6200 • FAX (415) 326-5512 • Telex 334486

REPORT DOCUMENTATION PAGE

Form Approved OMB No. 0704-0188

1. AGENCY USE ONLY *(Leave blank)*	2. REPORT DATE	3. REPORT TYPE AND DATES COVERED
	January 1992	Final Report 15 Nov 88 - 14 Nov 91

4. TITLE AND SUBTITLE
Excited Negative Ions and Molecules and Negative Ion Production (U)

5. FUNDING NUMBERS
61102F
2301A7

6. AUTHOR(S)
Jmes R. Peterson

7. PERFORMING ORGANIZATION NAME(S) AND ADDRESS(ES)
SRI International
333 Ravenswood Avenue
Menlo Park, CA 94025

8. PERFORMING ORGANIZATION REPORT NUMBER
MP 91-275

9. SPONSORING/MONITORING AGENCY NAME(S) AND ADDRESS(ES)
Air Force Office of Scientific Research
Building 410
Bolling Air Force Base
Washington, DC 20332-6448

10. SPONSORING/MONITORING AGENCY REPORT NUMBER
F49620-89-K-0002

11. SUPPLEMENTARY NOTES

12a. DISTRIBUTION/AVAILABILITY STATEMENT
Approved for public release; distribution unlimited.

12b. DISTRIBUTION CODE
UL

13. ABSTRACT *(Maximum 200 words)*

Research has been performed to determine fundamental properties of negative ions; decay mechanisms and products of molecular Rydberg states; and mechanisms affecting H^- production in ion source discharges. Experiments were performed on both stable and metastable states of Ca^-, Cs^-, He_2^-, and WO_3^-; on the dissociative decay of Rydberg states of H_3, D_3, D_2H, H_2D, NeH, NeD, NH, CH, and O_2; on the product states of dissociative recombination of Ar_2^+ and Kr_2^+; and on the vibrational distribution of O_2^+ resulting from the reaction $O^+ + CO_2 \rightarrow O_2^+ + CO$.

14. SUBJECT TERMS	15. NUMBER OF PAGES
Negative Ions, Molecular Rydberg States, Predissociation	68
	16. PRICE CODE

17. SECURITY CLASSIFICATION OF REPORT	18. SECURITY CLASSIFICATION OF THIS PAGE	19. SECURITY CLASSIFICATION OF ABSTRACT	20. LIMITATION OF ABSTRACT
Unclassified	Unclassified	Unclassified	SAR

NSN 7540-01-280-5500

Standard Form 298 (Rev. 2-89)
Prescribed by ANSI Std 239-18
298-102

CONTENTS

RESEARCH OBJECTIVES

The objectives of this work included determination of (1) fundamental properties of negative ions, (2) mechanisms of H^- production in volume discharge sources, and (3) properties and the decay mechanisms and products of molecular Rydberg states. These objectives are part of the larger goal of understanding the detailed behavior and properties (observables and other parameters that are needed for diagnostics) of the low density plasmas in the earth's ionosphere, negative ion sources, etching plasmas, and gas-based lasers.

ACCOMPLISHMENTS DURING THE CONTRACT PERIOD

1. PROPERTIES OF THE METASTABLE EXCITED $4S4p^2\ ^4P$ STATE OF Ca^-

We made the first confirmation of the existence of this ion, which had been predicted theoretically in 1982. We measured its decay lifetime to be 0.29 ± 0.1 ms and its energy to be 1.337 ± 0.050 eV above Ca ^1S; thus, the electron affinity of its parent state, Ca $4s4p\ ^3P$, is 0.562 ± 0.005 eV. A report of this work was published in Phys. Rev. Lett. **63**, 368 (1989).

2. DISSOCIATIVE DECAY OF NeH AND NeD RYDBERG STATES: A STRONG ISOTOPE EFFECT

The spectra of kinetic energies released in the radiative and predissociative decay of the three lowest Rydberg states of NeH and NeD were measured using our negative ion translational spectroscopy technique. These lowest bound states of NeH were formed by electron capture from Cs vapor by a 5 keV NeH^+ beam. The expected predissociation of A $^2\Sigma^+$ and the radiative decay of B $^2\Pi$ were both observed in NeH; however, a surprisingly strong suppression (by a factor of over 100) of the predissociation was found in the lower vibrational levels of NeD. This effect was deduced[1] to result from a reduced overlap of the bound and continuum nuclear wave functions of the Rydberg and ground electronic states, respectively. The results were published in J. Chem. Phys. **91**, 6880 (1989). They have stimulated some recent calculations,[2] which support them.

3. SHALLOW WELL IN THE GROUND STATE OF H_3O

Our work on NeH was first stimulated by experimental findings elsewhere that had been interpreted to indicate the presence of a shallow well in the ground state, which could provide metastable decay of NeD. After considerable effort, our work showed conclusively that those observations were caused instead by D_3O^+ contamination in the NeD^+ parent beam, which was undetected by mass analysis (same m = 22 amu). Moreover, our kinetic energy release spectra from both H_3O and D_3O produced from the parent ion beams by electron capture in Cs agreed with the existence of a shallow well in the ground H_3O state and with the energy level of about 1 eV predicted by recent calculations of Saxon and Talbi[3] (also at SRI) under a contract from AF Phillips Laboratory/Propulsion Directorate. This well results from the Rydberg nature of the ground state at small internuclear separations. These results will be submitted for publication in the Journal of Chemical Physics.

4. ELECTRON AFFINITY OF TUNGSTEN TRIOXIDE

Molecules of high electron affinity have been of interest for two decades because they have the ability to trap free electrons and thus find applications in the control of electron densities in reentry wakes and rocket exhausts, in rapid high-current switching, and in similar uses. WO_3 is one of the refractory metal oxides in this class of molecules, which present serious problems in the determination of their electron affinities. With partial support from Lockheed Missiles and Space Co., we built, tested, and and used a slow electron detector to measure photodetached electrons at several photon energies in the vicinity of the photodetachment threshold. We thus made the first direct determination of the electron affinity of WO_3, and found it to be 3.33 +0.08, -0.15 eV. (Previous indirect measurements had found values of 3.6 ± 0.4 and 3.9 ± 0.2 eV). This is probably the largest electron affinity that has been measured directly by photodetachment. The results were published in J. Chem. Phys. **95**, 824 (1991). Communications with Dr. John F. Paulson, AF Phillips Laboratory/Geophysics Directorate, Hanscom Air Force Base, showed that our results were very useful in some Air Force applications.

5. PREDISSOCIATION OF H_3 n = 2 RYDBERG STATES: PRODUCT BRANCHING AND ISOTOPE EFFECTS

Under the previous contract (No. F49620-85-K-0017) we had begun studies of the decay of H_3 Rydberg states produced by electron capture of H_3^+ in Cs because of their possible influence in the production of H^- in ion sources. We had found that the decay leads to both two-body (H + H_2) and three-body (H + H + H) products. Under the current contract, we have used our negative-ion translational spectroscopy technique to determine the product branching ratios and energy distributions from the decay of H_3, D_3, and HD_2. We also used two different ion sources to produce the parent ion beams, and to investigate the effects of internal rovibrational energy on these characteristics, and we have compared the results with very recent calculations and with the branching ratios from dissociative recombination of H_3^+, which is a similar process that occurs among much higher Rydberg states near the ionization continuum. The comparison suggests that the 3-body/2-body ratio increases monotonically with total internal energy (electronic plus rovibrational). The results have been submitted for publication in the Journal of Chemical Physics. A preprint is included as Appendix A.

6. RECENT DETERMINATIONS OF THE ELUSIVE PROPERTIES OF Ca^- $4s^24p\ ^2P$

The $4s^2$ closed-subshell character of ground state Ca was originally considered to have a negative electron affinity, i.e., it could not form a negative ion, in contrast to the strong electronic affinity, predicted theoretically for the first excited Ca 4s4p ^3P state resulting in the metastable ^4P state discussed above. The surprising discovery in 1987 that the ^1S ground state had a positive electron affinity of about 43 meV, as determined both experimentally[4] and theoretically,[5] precipitated our work on the metastable ^4P state described in (section 1) above. In that work we had found no evidence of the ^2P state in our beam, but in 1990 we undertook new experiments; not only did these experiments confirm the presence of the ^2P state, but photodetachment near the Ca ^3P + kp threshold indicated an electron affinity (EA) of only about 15 meV, compared to the previous experimental value of 43 ± 7 meV obtained at Oak Ridge National Laboratory.[4] This discovery, in the light of other new information from Paul Burrow's group at the University of Nebraska, caused considerable concern about our previous results and made further measurements at higher photon energies extremely important. Fortunately, after considerable effort we succeeded, and we found a large shape resonance near 3.0 eV, just above the ^1P + kp threshold. We made use of a formula that we had developed earlier in our work on He^- to analyze the data near the $4s4p^2\ ^4P$ shape resonance.[6] This formula gives a modified expression to the usual Wigner threshold law, to include the effects of a p-wave shape resonance, and permits accurate determination of the threshold and, in addition, yields the actual energy and width of the resonance, which are very important to electron scattering phenomena. We found a new value for the electron affinity, EA(Ca ^1S) = 18.4 ± 2.5 meV, which is in agreement with the less accurate value of 15 ± 6 meV obtained from the analysis of the lower ^3P threshold. That work is described in a paper recently submitted to Physical Review Letters, which is attached as Appendix B. A preliminary abstract was submitted for a poster session in the International Joint Symposium on Electron and Ion Swarms and Low Energy Electron Scattering at Bond University, Queensland, Australia, in July 1991, and it was upgraded to an invited paper, which paid the cost of Dr. Peterson's transportation to Australia.

In addition to the results just mentioned, we have also obtained beautiful data surrounding a strong interference minimum near 1.0 eV, which has only recently been found theoretically.[7] We also found additional proof that the metastable ^4P Ca^- state exists and obtained a binding energy EA(Ca ^3P) = 566 ± 6 meV, compared with the original theoretical value of 550 meV and with our first measurement of 562 ± 5 meV.[8] An extensive paper on our complete work on Ca^- will be submitted to Physical Review A.

With the new low value of the binding energy of 18 meV for the $Ca^- {}^2P$ ground state, the possibility of photodetachment by the 300 K blackbody radiation in our apparatus becomes an interesting question. We have calculated an approximate detachment lifetime of about 1 ms, using the theoretical cross sections calculated by Fischer and Hansen,[7] but this value is probably high because the wave functions they used predicted a binding energy of 62 meV. As we found earlier that our composite beam has an effective lifetime of 0.3 ms, it is important to establish the effect of blackbody photodetachment on the large ^2P component. Our results have stimulated new theoretical work by at least four groups with whom we are in close contact by electronic mail, so the quality of the calculations should improve.

7. PRODUCTION OF H^- IN Cs-SEEDED AND PURE H_2 DISCHARGE ION SOURCES

Our initial work[9] on the dissociative electron capture of H_3^+ in Cs was intended to explore the importance of this reaction in the production of H^- in Cs-seeded discharges, which is related to the production of energetic neutral H beams for applications in both directed energy weapons and heating plasmas in magnetic fusion energy tokamaks. It is now recognized that the predominant mechanism for forming H^- in H_2 discharges (plasmas) is dissociative attachment from highly vibrationally excited H_2. Our work has shown that the two-body decay of n = 2 Rydberg states of H_3 resulting from H_3^+ + Cs reactions is an important source of $H_2(v > 4)$ in cesiated discharges. The work also infers the importance of dissociative recombination of H_3^++ in pure H_2 discharges as a source of H_2 ($v > 4$). A paper on our analysis of the Cs-seeded discharges was published in SPIE **161**, 578 (1989), "Microwave and Particle Beam Sources and Directed Energy Concepts."

8. DISSOCIATIVE DECAY OF RYDBERG STATES OF C_2, CH, AND NH

In research similar to our work on HeH, NeH, H_3, etc., we carried out exploratory measurements on these other excited radicals of interest in flames and rocket exhausts. We obtained kinetic energy release spectra for all of them, but their interpretation was complicated, largely because of the relative paucity of good calculations of the excited state potentials. We have made a reasonable analysis of the NH data, which will be prepared for publication in the Journal of Chemical Physics.

9. SEARCH FOR THE $^4P \rightarrow {}^4S$ RADIATIVE TRANSITION IN Ca^-

This bound-bound transition has been predicted theoretically (one of the very few such transitions in negative ions), and we have attempted to find it near its predicted location of 442 nm.

Direct photodetachment is not allowed, but the transition lies in the continuum of lower photodetachment thresholds. We tried to detect it from an expected change in the combined autodetachment and collisional detachment rate, compared to those of the lower ^4P state, to alter the photodetached signal. Although this resonant line is fully allowed and probably has nearly unit oscillator strength, detection of the resonantly scattered radiation from the beam is probably too difficult in our apparatus because of the background from laser light scattered by collimating apertures and windows, so we relied on this secondary method of detection. We searched over a fairly broad energy range without success. The failure so far may have resulted from inaccuracies in the calculated position of the transition or from the relatively small fraction of the beam in the ^4P state compared to the ^2P ground state Ca^-. Further calculations are being undertaken by C. F. Bunge of the National University of Mexico, who did the original theoretical work.

10. FINAL PRODUCT STATES OF Ar_2^+ DISSOCIATIVE RECOMBINATION

An analysis was made of an anomalous superthermal peak in the velocity distribution of metastable Ar^* obtained from an Ar discharge by Hardy et al.[10] The authors had concluded that the extra peak was caused by Ar^- formed in the discharge, and they sent Dr. Peterson a preprint for comments (we had first observed Ar^- in our previous contract[11]). The very short (0.3 ms) lifetime[11] of Ar^- essentially prevents Ar^- from participating, but from the variations of relative intensity of the peak with changes in pressure, and the absence of changes in its location with discharge conditions, it appeared very likely that the peak was caused by fast Ar^* products of dissociative recombination of Ar_2^+ : $Ar_2^+ + e \rightarrow Ar^* + Ar$. The authors then sent more of their original data for further analysis, and from the time-of-flight data, it was easy to conclude that the excited Ar^* products are primarily in the 4s states instead of the 4p states that are commonly believed (in the gaseous electronics and rare gas excimer laser community) to be the excited products. Only about 10% or less of the reactions yield 4p states. Dr. Peterson suggested additional measurements using Kr gas. They found a similar peak, which Dr. Peterson analyzed, about 80% of the products were Kr (5s) and 20% (5p), whereas the accepted belief was that a population of 100% 5p atoms. A poster at the recent Gaseous Electronics Conference in Albuquerque drew a reprint request list that totaled about 15% of the conference registrants. A short paper will be written jointly with the original authors to disclose the results, for publication in the Journal of Chemical Physics.

11. CONSTRUCTION OF A COOLED HOLLOW CATHODE ION SOURCE

This new ion source, which was built to produce molecular ions that are rovibrationally cool, has proved very effective. Its use during the H_3^+ + Cs dissociative charge transfer experiments proved crucial to the proper interpretation of the kinetic energy release spectra.

In experiments in Amsterdam (to be discussed in section 14 below), the new source was found capable of yielding O_2^+ beams completely in v = 0.

12. SEARCH FOR METASTABLE Cs^- ^3P

A recent calculation by Greene[12] predicted the existence of a bound 6s6p ^3P state of Cs^-, located 18 meV below the 6s ^2S state of Cs and 454 meV above the $6s^2$ ^1S ground state of Cs^-. We sought evidence of this excited state in a Cs^- beam produced by electron capture by Cs^+ ions in Cs vapor, by laser photodetachment near the threshold of the Cs 5d ^2D + ks channel, predicted to occur near 14625 cm^{-1}. Although our Cs^- beam should be primarily in the well-bound ^1S ground state, we hoped that the structure from this channel would be visible on the lower shoulder of the known[13] Feshbach resonance below the Cs^- $^1S \rightarrow$ Cs 6p ^2P + kp threshold at 14981 cm^{-1}. We used our slow electron detector and clearly saw the Feshback resonance, but any structure on its lower side was lower than the noise level. We have since learned that new calculations have found that this predicted odd-parity state is unbound.

13. PHOTODETACHMENT OF He_2^-

We had first discovered this unpredicted metastable highly excited ion under an earlier contract, No. F49620-85-K-0017) measured its lifetime,[14] and studied its autodetachment spectrum;[15] however, the beams were always too weak for photodetachment experiments. The new cooled hollow cathode ion source has proved so efficient in forming He_2^- that we are now able to make photodetachment measurements on this unusual ion for the first time. This increased efficiency undoubtedly occurs because rovibrationally cold He_2^- ions do not rapidly autodetach to form their He_2 $a^3\Sigma_u^+$ Rydberg parents. Only v = 0 is actually bound with respect to $a^3\Sigma_u^+$. We have made initial measurements in the 1.8-2.5 eV range but have seen no evidence of resonance structure, only what appears to be the tail of a larger structure at lower energy. We plan additional measurements at lower energies. We will use the new Ti:sapphire laser recently acquired with partial funding from the National Science Foundation (NSF).

14. FINE-STRUCTURE DISTRIBUTIONS AMONG THE ^3P PRODUCTS OF O_2 $d^1\Pi_g$ (v = 0) PREDISSOCIATION

In October 1990, Dr. Peterson went to the FOM Institute for Atomic and Molecular Physics (AMOLF) in Amsterdam, with support from a NATO travel grant and a stipend from AMOLF. We pursued details of some work we had done there during the previous contract, on the predissociation of O_2 3s $^{1,3}\Pi_g$ Rydberg states.[16-19] We formed the Rydberg states in fast beams produced from the parent O_2^+ ions by electron capture in Cs. We have shown that this process very closely reproduces in the Rydberg molecules the rovibrational distribution of the initial ions. In Amsterdam we used a copy of our SRI cold hollow cathode ion source (cooled to liquid nitrogen temperature) and were able to obtain the 3s $d^1\Pi_g$ and $C^3\Pi_g$ Rydberg molecules in v = 0 only, and also found that the rotational temperature was much colder than in the previous work. These characteristics allowed the determination of the distribution of the three J = 0-2 fine structure states of ^3P products in the $^1P + {}^3P$ predissociation channel. We were able to conclude that the Ω = 0-2 distribution in the initial $C^3\Pi_g$ Rydbergs is passed on to the J = 0-2 products, which have undergone an avoided crossing in the dissociating state. These details cannot be seen by any other technique. A paper is in preparation for publication Chemical Physics Letters.

15. CONSTRUCTION OF A NEW Cs OVEN FOR HIGH RESOLUTION MEASUREMENTS OF RYDBERG MOLECULE DECAY PRODUCTS

A small alkali vapor oven has been constructed for use on the apparatus; it is equipped with a time- and position-sensitive coincidence detector to permit the high resolution measurements of the c.m. kinetic energies released in dissociative decay of molecular Rydberg states. Such measurements have previously been possible only in Amsterdam. The oven is capable of being moved out of the ion beam and returned to its original aligned position with great precision. It has been tested on O_2 Rydberg decays and has been used for new measurements as described below.

16. DETERMINATION OF THE VIBRATIONAL DISTRIBUTION IN O_2^+ PRODUCED IN THE REACTION $O^+ + CO_2 \rightarrow O_2^+ + CO$

We were strongly motivated to make these measurements by conversations with Dr. John F. Paulson of AF Phillips Laboratory/Geophysics Directorate, Hanscom Air Force Base, who described their importance to current Air Force problems. The vibrational products of this reaction, which is 1.19 eV exothermic, have importance in rocket exhausts and chemical releases in the earth's ionosphere,[20] and in the ionospheres of Mars and Venus. In these regions this reaction is rapidly followed by dissociative recombination, $O_2^+ + e \rightarrow O$ (^3P or ^1D) + O (^3P, ^1D, or ^1S),

which leads to a rapid depletion of the electrons in the F region of the earth's ionosphere, where the dominant ion is atomic O^+, which recombines very slowly. Both the reaction rate and products are strongly influenced by the vibrational state of the O_2^+ reactant. The only previous determination of the vibrational products was obtained recently by Viggiano et. al,[20] using an indirect method.

We used an electron impact ion source with pure CO_2 gas to produce O_2^+ by the reaction $e + CO_2 \rightarrow O^+ + CO$ followed by the title reaction. (O_2^+ is not produced directly from CO_2 by electron impact.) The reaction product O_2^+ ions were extracted from the source, accelerated to 3 keV, focussed, collimated, and directed into the new Cs oven described above. The $^{1,3}\Pi_g$ Rydberg states of our previous studies are efficiently formed by electron capture and decay rapidly within the small cell, and the products are detected downstream by the arrival time- and position-sensitive detector. The output signals are processed by an on-line computer, which converts the data into c.m. kinetic energy release spectra; these spectra display the vibrational distributions in the Rydberg molecules, which are virtually identical with those in the initial O_2^+ beam. This technique thus gives essentially a direct measurement of the distribution in the ions, whereas the previous technique[20] was fairly indirect and more approximate.

Preliminary data were submitted to the July 1991 International Conference on the Physics of Electronic and Atomic Collisions (ICPEAC). The abstract is included as Appendix C. More refined data have been taken and are still being analyzed. Essentially, we find levels populated from v = 0-6. Only the distribution among v = 0-2 was determined by Viggiano et al.[20] This distribution is in rough agreement with our direct results but does not agree in detail. We also obtain the approximate rotational distribution from each vibrational level. We find that the rotational temperature decreases significantly as v increases. This effect probably follows the rationale: The total exothermicity is fixed, ~1.19 eV, and the initial ions are nominally thermal (we see some effects indicating a small exothermal content). Thus, as v increases in O_2^+, less translational energy is given to the $O_2^+ + CO$ reaction products, and thus less linear impulse, and less rotational excitation in the O_2^+ occurs. We hope to explore this and similar reactions in the future using this technique. A paper reporting the results of these measurements will be submitted shortly to the Journal of Chemical Physics and will acknowledge the support of AFOSR.

PUBLICATIONS DURING THE CONTRACT

1. W. J. van der Zande, W. Koot, J. Los, and J. R. Peterson, "$O_2^+(a^4\Pi_u)$ Collisions with Cs and Mg: Formation of $(3s\sigma g)\ ^{3,5}\Pi_u$ Rydberg and Repulsive Valence States of O_2," Chem. Phys. **126**, 169 (1988).

2. W. J. van der Zande, W. Koot, J. Los, and J. R. Peterson, "Predissociation of 3s $^{1,3}\Pi_g$ and $^{3,5}\Pi_u$ Rydberg States of O_2: Mechanisms and Pathways," in *Dissociative Recombination: Theory, Experiment and Applications,* J.B.A. Mitchell and S. L. Guberman, Eds. (World Scientific Publishing Co., 1989), pp. 162-174.

3. J. R. Peterson, W. G. Graham, and P. Devynck, "Mechanisms for H^- Production in Cs^--seeded Ion Sources," Proc. SPIE **1061**, 578 (1989).

4. D. Hanstorp, P. Devynck, W. G. Graham, J. R. Peterson, and J. Los, "Observation of Metastable Autodetaching Ca^-," Phys. Rev. Lett. **63**, 368 (1989).

5. P. Devynck, W. G. Graham, and J. R. Peterson, "Dissociative Decay of NeH and NeD Rydberg States: A Strong Isotope Effect," J. Chem. Phys. **91**, 6880 (1989).

6. H. H. Michels, R. H. Hobbs, Y. K. Bae, and J. R. Peterson, "Comment on 'An Experimental and Theoretical Study of the Negatively Charged Helium Dimer, He_2^-,'" Chem. Phys. Lett. **170**, 411 (1990).

7. C. W. Walter, Ch. Hertzler, P. Devynck, G. P. Smith, and J. R. Peterson, "Photodetachment of High Electron-Affinity Negative Ions," Nucl. Instr. Math. Phys. Rev., B**56/57**, 216 (1991).

8. C. W. Walter, Ch. Hertzler, P. Devynck, G. P. Smith, and J. R. Peterson, "Photodetachment of WO_3^-," J. Chem. Phys. **95**, 824 (1991).

9. J. R. Peterson, P. Devynck, Ch. Hertzler, and W. G. Graham, "Predissociation of H_3 n = 2 Rydberg States: Product Branching and Isotope Effects," submitted to J. Chem. Phys. (1991). See Appendix A.

10. C. W. Walter and J. R. Peterson, "A Shape Resonance in Ca^- Photodetachment and the Electron Affinity of $Ca(^1S)$," submitted to Phys. Rev. Lett. (1991).

11. C. W. Walter, Ch. Hertzler, and J. R. Peterson, "Photodetachment of the Weakly Bound ^2P and Metastable ^4P States in Ca^-," to be submitted to Phys. Rev. A. See Appendix B.

12. J. R. Peterson, K. A. Hardy, and J. W. Sheldon, "Final States of Dissociative Recombination in Ar_2^+ and Kr_2^+," to be submitted to J. Chem. Phys.

13. C. W. Walter, P. C. Cosby, and J. R. Peterson, "Ro-vibrational Distribution in O_2^+ from $O^+ + CO_2$ Reactions," to be submitted to J. Chem. Phys. See Appendix C.

PROFESSIONAL PERSONNEL AND INTERACTIONS

PERSONNEL

The primary contributors to this research were Dr. James R. Peterson, Principal Investigator; Dr. Pascal Devynck and Dr. C. Wesley Walter, Postdoctoral Research Associates; and Dr. Christoph Hertzler, a postdoctoral Visiting Scientist from the University of Kaiserslautern, Germany, who was supported by a Deutsche Forschungsgemeinschaft grant, and received a stipend from a National Science Foundation grant. In addition, early contributions were made by Prof. William G. Graham, on sabbatical leave from the University of Ulster, N. Ireland; and by Dag Hanstorp, a graduate student from Chalmers University of Technology, Goteborg, Sweden, who was supported by a grant from Sweden. Local experimental contributions were made by Dr. Philip C. Cosby, and we were aided theoretically by Dr. David L. Huestis and Dr. Roberta P. Saxon, all of the Molecular Physics Laboratory of SRI.

COLLABORATIONS

In October and November 1990, J. R. Peterson spent five weeks at the FOM (Foundation for Research on Matter) Institute for Atomic and Molecular Physics in Amsterdam, The Netherlands, working with Dr. W. J. van der Zande. This work is described in Section 14 of the Accomplishments. Support came from a NATO travel grant and a stipend from the FOM. Dr. Peterson was also invited to present seminars at the University of Freiburg and the University of Kaiserslautern in Germany. We have also collaborated with Profs. K. A. Hardy and J. W. Sheldon, Miami International University, in analyzing their results, as described in Section 10 of the Accomplishments.

PRESENTATIONS

Eleven contributed papers were presented at different conferences: the Gaseous Electronics Conference (three papers), the APS Division of Atomic, Molecular and Optical Physics-DAMOP (four papers), and the International Conference on the Physics of Electronic and Atomic Collisions (four papers).

Two invited papers were presented, one at the 11th International Conference on the Applications of Accelerators in Research and Industry, Denton, Texas, 5-8 November 1990; and

one at the Joint Symposium on Electron and Ion Swarms and Low Energy Electron Scattering, Bond University, Queensland, Australia, 18-20 July 1991.

Colloquia were given at the University of Nevada, Reno, at the FOM Institute for Atomic and Molecular Physics, Amsterdam, The Netherlands; at the University of Freiburg, Germany; and at the University of Kaiserslautern, Germany.

REFERENCES

1. P. Devynck, W. G. Graham, and J. R. Peterson, J. Chem. Phys. **91**, 6880 (1989).

2. I. D. Petsalakis, T. Mercouris, G. Theodorakopoulos, and C. A. Nicolaides, J. Chem. Phys. **93**, 6642 (1990).

3. D. Talbi and R. P. Saxon, J. Chem. Phys. **91**, 2376 (1989).

4. D. J. Pegg, J. S. Thompson, R. N. Compton, and G. D. Alton, Phys. Rev. Lett. **59**, 2267 (1987).

5. C. Froese Fischer, J. B. Lagowski, and S. H. Vosko, Phys. Rev. Lett. **59**, 2263 (1987).

6. J. R. Peterson, Y. K. Bae, and D. L. Huestis, Phys. Rev. Lett. **55**, 692 (1985).

7. C. Froese Fischer and J. E. Hansen, Phys. Rev. A **44**, 1559 (1991).

8. D. Hanstorp, P. Devynck, W. G. Graham, and J. R. Peterson, Phys. Rev. Lett. **63**, 368 (1989).

9. J. R. Peterson and Y. K. Bae, Phys. Rev. A **30**, 2807 (1984).

10. K. A. Hardy, E. Gillman, and J. W. Sheldon, J. Appl. Phys. **67**, 7240 (1990).

11. Y. K. Bae, J. R. Peterson, A. S. Schlachter, and J. W. Stearns, Phys. Rev. Lett. **54**, 789 (1985).

12. C. H. Greene, Phys. Rev. A **42**, 1405 (1990).

13. T. W. Patterson, H. Hotop, A. Kasden, D. W. Norcross, and W. C. Lineberger, Phys. Rev. Lett. **32**, 189 (1974).

14. Y. K. Bae, M. J. Coggiola, and J. R. Peterson, Phys. Rev. Lett. **52**, 747 (1984).

15. Y. K. Bae, J. R. Peterson, H. H. Michels, and R. H. Hobbs, Phys. Rev. A **31**, 2778 (1988).

16. W. J. van der Zande, W. Koot, J. R. Peterson, and J. Los, Chem. Phys. Lett. **140**, 283 (1987).

17. W. J. van der Zande, J. R. Peterson, W. Koot, and J. Los, J. Chem. Phys. **89**, 6758 (1988).

18. W. J. van der Zande, W. Koot, and J. Los, J. Chem. Phys. **91**, 4597 (1989).

19. W. J. van der Zande, W. Koot, J. Los, and J. R. Peterson, Chem. Phys. **126**, 169 (1988).

20. A. A. Viggiano, R. A. Morris, F. Dale, and J. F. Paulson, J. Chem. Phys. **93**, 1681 (1990).

Appendix A

PREDISSOCIATION OF H_3 n = 2 RYDBERG STATES: PRODUCT BRANCHING AND ISOTOPE EFFECTS

PREDISSOCIATION OF H_3 n = 2 RYDBERG STATES: PRODUCT BRANCHING AND ISOTOPE EFFECTS

J. R. Peterson, P. Devynck, Ch. Hertzler, and W. G. Graham
Molecular Physics Laboratory
SRI International, Menlo Park, CA 94025 USA

ABSTRACT

A translational spectroscopy technique is used to obtain predissociation kinetic energy release spectra from the lowest bound states of H_3, 2s $^2A_1'$ and 2p $^2A_2''$. These H_3^* states are formed in near-resonant electron capture by 3 keV H_3^+ in Cs vapor. Their ground rovibrational levels are energetically about 1 eV above the H + H + H dissociation limit, thus all levels can yield both H_2 + H and the 3-body products. The spectra contain both 3-body and 2-body components, and are deconvoluted to obtain the branching ratios. Data obtained from two different ion sources show that the 3-body/2-body ratio increases with increased rovibrational energy in the H_3^*. The results are compared to recent theory, and with previously reported ratios from dissociative recombination of H_3^+. The comparison suggests that the ratio increases monotonically with the total electronic and rovibrational energy in the H_3^*. D_3^* predissociation has a similar behavior. The H- and D-atom spectra from the 2-body decay of HD_2^* show that the ejected H-atom is strongly favored on a per-atom basis.

MP 91-135
August 2, 1991

I. INTRODUCTION

The triatomic radical H_3 is purely dissociative in its ground electronic state, but bound states exist when one of the electrons is in an excited Rydberg orbital. Such "Rydberg" molecules have recently been reviewed by Herzberg,[1] who gave considerable attention to H_3. Optical spectra have shown that the lowest bound state of H_3, 2s $^2A_1'$, predissociates in about 0.2 ps.[2] The nearby 2p $^2A_2''$ state, however, decays by rotational coupling with lifetimes of about 30 ps for rotational level N = 1, decreasing rapidly with rotational excitation.[2] However its rotationless (N = K = 0) lower symmetric stretch and bending states are stable against rotational predissociation.[3,4] Their slow decay was originally considered to be purely radiative, to 2s $^2A_1'$, with a calculated lifetime of about 87 μs.[3] However, recent measurements have found lifetimes in the 600-800 ns range,[5] with the more rapid decay attributed to (a) radiation directly to the ground state accompanied by bending-mode excitation, and (b) possibly some spin-orbit coupled predissociation.[5]

These two primarily predissociating H_3^* states lie about 1 eV above the H + H + H limit (see Figure 1), so the predissociation of each can produce both H + H + H and H_2 + H products. Until this work, there have been no measurements of the relative yields of the 3-body and 2-body products from these states. Peterson and Bae,[6] in a trial translational spectroscopy experiment, measured the D-atom energy distributions and yields from D_3^* formed by electron capture of D_3^+ in Cs, and noted both 2-body and 3-body products. Cosby and Helm[7] have examined predissociation of nearly rovibrationless levels of the 3s $^2A_2'$ and 3d $^2E''$ states produced by photoexcitation from the metastable 2p $^2A_2''$ levels. By detecting the radial positions and time differences in the arrival of the 2-body decay products in a fast beam experiment, they were able to obtain detailed vibrational distributions in the H_2 products, which extended strongly into the continuum.[7] They also found direct evidence of 3-body products, but they did not determine the relative yields. Mitchell et al.[8,9] have measured 3-body/2-body product branching ratios from the dissociative recombination of H_3^+ with low energy electrons:

$$H_3^+ + e \rightarrow H_3^* \rightarrow \text{neutral products.} \quad (1)$$

This is also a predissociative process, but it originates through very high n and transient vibrationally excited H_3^* Rydberg states whose total energies are just above the ionization limit, and the results will be discussed below.

In this paper, we report measurements of the branching ratios, energy distributions, and isotopic dependences of the dissociation products of the $n = 2$ Rydberg states of H_3, D_3, and HD_2. These states can be formed very efficiently from an H_3^+ beam by electron capture from Cs (I.P. = 3.89 eV) in the reaction

$$H_3^+ + Cs \rightarrow H_3^*(n = 2) + Cs^+ \quad (2)$$

because the reaction is nearly "resonant" (little change in total internal energy) and because the H_3^+ - H_3^* Franck-Condon factors are essentially unity for $\Delta v = 0$. The $\Delta v = 0$ reaction is endothermic by only 0.11 eV for the 2s $^2A_1'$ product and 0.22 eV for 2p $^2A_2''$. The near-resonant characteristic allows transitions at large impact parameters, and hence large cross sections.[10] The measured total cross section for Reaction (2) exceeds 150 Å^2 at ion beam energies below 3 keV.[10] Transitions to the directly dissociating 2p $^2E'$ ground state are strongly inhibited by very poor Franck-Condon factors.

The essentially diagonal nature of the Franck-Condon factors has another very important role in these experiments beyond assisting the formation of the Rydberg states. It results from the fact that the Rydberg states consist of the ion core plus a relatively noninteracting (higher n) electron. Because of this diagonality and the "softness" of the near-resonant collisions, the rovibrational distribution in the initial H_3^+ beam is strongly preserved in the H_3^* products of Reaction (2), as has been demonstrated in H_2^+ + Cs reactions.[11] The use of different ion sources allows us to vary the internal energy in the parent H_3^+ ions, and consequently in the H_3^*.

We have asserted that the H_3^* molecules formed in Reaction (2) in our experiment are predominantly in n = 2 Rydberg states. What about higher n states? The near-resonant selectivity is a strong condition at the intermediate collisional velocities of our experiments ($v \sim 4 \times 10^7$cm/s). Bound-bound radiation from n = 3 states of D_3 produced by electron capture of 5 keV D_3^+ beams in K vapor was observed by Figger et al.,[12] with an estimated partial cross section of $\sim 10^{-19}$ cm^2 for formation of D_3 molecules in n = 3 states. Considering that the total capture cross section is 10^{-14} - 10^{-15} cm^2,[12] it is probable that at least 99% of the products are in n = 2. We find no evidence to the contrary.

II. EXPERIMENTAL TECHNIQUE

The technique used to probe the nature of the dissociation products following electron capture in Cs has been described elsewhere.[6,13] We use a translational spectroscopy technique to obtain the distribution of total center-of-mass (c.m.) kinetic energies released to the dissociation fragments. This quantity, W, is the difference between the total internal energy (electronic and rovibrational) in the excited H_3^* before predissociation and of the final products. We utilize the fact that following the predissociation:

$$H_3^* \rightarrow H_2 + H, \tag{3a}$$

or

$$H_3^* \rightarrow H + H + H, \tag{3b}$$

a small fraction of the fast H products, produced from ~ 3 keV H_3^+ ions via Reactions (2) and (3), can capture an electron in a subsequent collision within the cesium oven, to form a negative ion:

$$H + Cs \rightarrow H^- + Cs^+ . \tag{4}$$

We then measure the laboratory kinetic energies of the H^- ions formed at 0° in the direction of the beam, which represent H atoms from (3) ejected from H_3^* at 0° and 180° c.m. angles. These data are then manipulated, as discussed below, to obtain the c.m. kinetic energy release spectrum P(W).

A. APPARATUS

A partial diagram of the apparatus is shown in Figure 2. H_3^+ ions are formed in an ion source (described below) from H_2, D_2, or mixtures of them, extracted and accelerated to the final beam energy, focused, mass selected by a magnetic field, and directed into a Cs vapor oven, where they undergo Reactions (1) to (3). H^- ions emerging from the oven along the beam axis pass into the analysis chamber, enter an electrostatic quadrupole deflector, Q1, where they are separated from the positive and neutral components, and are deflected 90° to the entrance of an energy analyzer. Neutrals leaving the oven pass directly through Q1 and into a Faraday cup, FC1, where they are monitored by their secondary electron current. The voltages on the deflecting quadrupole and the energy analyzer are coordinated to pass ions of the same energy. The ions that emerge from the energy analyzer enter a microchannel-plate detector (MCP) whose output pulses are directed to an on-line computer.

In this way, we effectively measure the laboratory energies of the H atoms from Reaction (3) that are ejected at c.m. angles very close to 0° and 180°. The ~3 eV laboratory energy lost in forming H^- in Reaction (4) is negligible in determining W. There is also a small amount of angular scattering[14,15] in Reaction (4), which reduces the energy resolution of the technique, but it does not affect the value of W.

To examine the effects of H_3^* internal excitation on the 3-body/2-body branching ratios, we have used two different ion sources. In our first experiments, a Colutron-type sustained discharge source was used, which produces rovibrationally hot H_3^+ ions. More recently, we have used a cooled hollow cathode source,[16] operating at about 1-3 Torr, which yields relatively cool ions. As mentioned above, the long-range nature of Reaction (2) and the diagonal nature of the ion-Rydberg

Franck-Condon matrix preserves the ion's internal energy distribution in the product Rydberg states, thus we can produce H_3^* internally "cool" using the hollow cathode and "hot" using the Colutron source. We will use data from the hollow cathode source to explain the data analysis.

B. DATA ANALYSIS

An example of the laboratory kinetic energy spectrum obtained from a 3.2 keV H_3^+ beam using the hollow cathode source is shown in Figure 3. The lower-energy half of the spectrum in Figure 3 represents H atoms ejected at 180° c.m. and the higher energies result from ejection at 0°. The laboratory data is analyzed according to the method previously used for HeH dissociation.[13] To obtain the c.m. kinetic energy release spectrum P(W), the data at laboratory energy E are first divided by the cross section at E for forming H^-, Reaction (4), using smoothed data from Miethe et al.[17] [Data from D^- measurements are divided by the H^- cross section at E/2, acknowledging the velocity dependence of Reaction (4)]. They are then divided by E itself because the energy analyzer is operated so that $\Delta E/E$ = constant. The c.m. solid angle subtended by the entrance aperture to the energy analyzer depends on the laboratory velocity of the particle detected and also the beam velocity, and has a cusp at W = 0, which creates the large central peak in Figure 3. The laboratory-to-c.m. solid angle transformation is expressed by the differential cross section for the isotropic breakup of a 2-body system into masses m_1 and m_2:[18]

$$d^2\sigma/dW d\Omega_c = (\mu/m_1)^{3/2} (W/E)^{1/2} d^2\sigma/dE_1 d\Omega_\ell \qquad (5)$$

where $\mu = m_1m_2/(m_1 + m_2)$, E is the laboratory energy of m_1 (the detected particle), W is the c.m. total kinetic energy of the fragments, and $d\Omega_c$ and $d\Omega_\ell$ are the c.m. and laboratory solid angles subtended by the detector. The value of W for each value of E of the data is determined from

$$W = (1 + m_1/m_2) (E^{1/2} - E_0^{1/2})^2, \qquad (6)$$

where $E_0 = E_B m_1/(m_1 + m_2)$ is the laboratory energy of m_1 when W = 0, and E_B is the beam energy. In the transformation program, when $E < E_0$, i.e., for atoms ejected at 180° c.m., W is assigned a negative value in order to separate and identify the two transformed data sets, which can subsequently be plotted independently. The corrections to the raw data mentioned above render the transformed 0° and 180° components quite symmetric in height, apart from some scattering effects. If they are not symmetric in W near W = 0 the original data are re-transformed using a new value of E_B, to correct for the plasma potential in the ion source, etc., which can change the beam energy by a few eV from that of the acceleration voltage. Changes of only a few eV in E_B have a strong influence in the spectra for small W ($\lesssim$ 1 eV). In this way zero of the W scale is obtained quite accurately. The energy scale for W obtained from the transformation is valid only for the 2-body case. The 3-body case is discussed below.

The transformed data from Figure 3 are shown in Figure 4. The solid line links the data from the higher energy part of the data in Figure 3, representing the 0° c.m. fragments, and the dots are the data from the lower energy (180° c.m.) part. The close agreement between the two data sets validates the data treatment procedure.

1. Deconvolution of the c.m. spectrum.

The P(W) spectrum in Figure 4 has two components; the higher energy peak is logically attributed to the 2-body products, and the lower one to the 3-body component. To obtain the branching ratios, the total spectrum must be deconvoluted in some reasonable way without an accurate knowledge of the relative shapes of the two individual distributions. Our procedure evolved during the course of the work, and was finally settled with the aid of the data from the hollow cathode source. The deconvolution is simpler for the laboratory spectra obtained from the "cold" ions, and is demonstrated using the 0° and 180° data from Figure 4, which have been combined and smoothed in Figure 5. We first note that the 2s and 2p states of H_3 are 0.97 and 1.08 eV above the H_2 dissociation limit, thus the *lower limit* to the 2-body spectrum is about 1.0 eV. Also, we expect the ejected H_2 molecules to have a vibrational population extending into

the continuum, since the 3-body products are observed. In Figure 5, we note that the full spectrum has a rather narrow low-energy peak, and then begins to diverge (toward the higher peak) at ~1eV, where it begins to receive contributions from the low-energy tail of the 2-body distribution. We then draw a short straight line tangent to the total envelope at the point of divergence. Next, we note that the high-energy peak deviates toward the low-energy peak at about 4.2 eV. Another straight line is drawn here tangent to the full curve, and subtracted from it to yield the terminus of the high-energy tail of the 3-body spectrum, as shown in dashes. With the expectation that the 3-body spectrum should not show any substructure, a smooth curve is then drawn monotonically from the dashed line, to join the lower tangent line just above 1 eV. This curve is then subtracted from the total to yield the 2-body spectrum. After several tries, a "reasonable" deconvolution is obtained, which does not contain any sharp substructure in either distribution. The different variations produce only minor changes in the areas.

It is also worth noting that the upper limit to the 2-body distribution for robvibrationless H_3^* is 5.5 eV. Higher values of W in the spectrum result from internally excited H_3^*, and also from the bandwidth ΔE of the energy analyzer, which results in $\Delta W \alpha W^2$.

In contrast to the hollow cathode source data, deconvolution of the spectra obtained using the hot discharge source was much less obvious. Figure 6 shows the c.m.-transformed data from H_3^+ formed in the Colutron ion source. The low-energy peak is considerably wider and relatively larger in area than in the hollow cathode case. Both aspects result from increased internal energy in the H_3^+ ions, and consequently in the Rydberg products of Reaction (2). More highly excited H_3^* molecules clearly yield a more dominant and broader 3-body component. In addition, the 2-body spectrum is pushed to higher energies. As the internal energy in H_3^* increases, both the upper and lower limits of the 2-body spectrum, corresponding respectively to the H_2 in $v = 0$ and at its dissociation limit, are increased in energy. Another version of a deconvolution of the Colutron data, with a slightly more prominent low-energy 2-body tail somewhat resembling that from the

hollow cathode source, was also used and the two results (only slightly different) were averaged in obtaining the branching ratio.

2. Determination of the 3-body/2-body branching ratio.

The absolute energy scale is important in determining the W values in the two distributions, but as will be explained below, it does not affect the determination of the branching ratios, which depend only on the areas under the two distributions. The reason for this independence of scale is that initially the spectra are obtained in the laboratory energies, and only one particle is detected per predissociation event; the other fragments have different energies and/or directions, and are not detected. The probability of an ion passing through the energy analyzer depends only on (a) its laboratory energy, because of the energy dependence of the analyzer bandwidth, and (b) its laboratory velocity relative to the velocity of the parent molecule, because of the laboratory-c.m. solid angle transformation. Thus the detection probability is independent of the masses or velocities of the other fragments, which are considered in determining W.

Although the branching ratios can be determined from the areas under the two distributions using the 2-body scale, we must account for the multiplicity of the *detected* atoms among the fragments. Since three H atoms in H_3 are ejected in a 3-body event, and only one in a 2-body event, only 1/3 of the area under the 3-body peak corresponds to individual events, compared to the area under the two-body distribution. If we measure D^- from HD_2, we use 2/3 of the area under the 3-body peak to compare with the full area under the 2-body peak, and if we detect H^- from HD_2, we use the full 3-body area.

With the 3-body peak area properly weighted by the inverse of the multiplicity of the detected H or D atom among those ejected (the relative probability of detecting a single event) the resulting areas under the two distributions are proportional to the number of dissociation events in each channel.

3. Determination of energy scale for W.

The energy scale of Figs. 4-6 is exact for the 2-body spectra. The 3-body scale can only be determined for fixed dissociation geometries. As earlier,[6] we use three simple cases as examples in the c.m. system. The first is identical to the 2-body case, except that two *unbound* atoms leave with the same velocities, with the third in the opposite direction. In the second, one atom is at rest and the others have opposing momenta. The energy scale for this case is 4/3 times the 2-body scale. In the third case, the three atoms depart symmetrically, at 120° to each other, with equal momenta. The scale for this case is 2 times the 2-body scale. The actual distribution of geometries will encompass all of these prototypes. The average geometry is unknown. In recent wave-packet studies of predissociation in H_3 Rydberg states, Orel and Kulander[19] found that the 3-body products tend to favor a collinear geometry, with one atom between two widely separated ones. With this finding in mind, we have weighted the first two cases equally, and the third with 1/2 their individual probability, in the order 2:2:1, yielding the average 3-body scale of 1.33 times the 2-body scale. This scale is used in determining the average energy of the 3-body distribution as described next.

4. Estimate of the internal energy in the H_3^*.

To estimate the internal energies in the H_3^* molecules that yielded the measured kinetic energy distributions, we assumed that the average W in the 3-body distributions was equal to the average total internal (electronic plus rovibrational) energy in the H_3^* n = 2 distributions, relative to the H + H + H asymptotic limit of 4.48 eV above the H_2 + H ground state. This energy consists of 1.0 eV of electronic energy plus the average rovibrational energy. The average W values in the 3-body distributions were obtained directly from the deconvoluted spectra using the 1.33 scaling factor and $W_{av} = \int WP(W)dw / \int P(W)dW$.

Although this model is somewhat arbitrary, it is based on logical assumptions with theoretical guidance, it is the best that we could conceive, and it is probably accurate within the

ample acknowledged uncertainties. An experimental determination is impossible because the states are so rapidly predissociated (except for the negligible metastable rotationless 2p states). For the present work, we felt that it was appropriate to use the average W in the 3-body distribution as an estimate of the internal energy in the H_3^* Rydberg states before they predissociate.

III. RESULTS

A. Branching ratios.

The 3-body/2-body branching ratios were found to increase with the internal energy in the H_3^* Rydberg states, as determined from the average c.m. kinetic energies in the 3-body distributions. These ratios are plotted in Figure 7.

We found that the average energies in the 3-body distributions from the cooled hollow cathode source were about 1.48 ± 0.15 eV for H_3 and 1.52 ± 0.15 eV for D_3, and the 3-body/ 2-body ratios were 0.23 ± 0.02 and 0.35 ± 0.02, respectively. Evidently the internal energies in the D_3^+ ions were only slightly higher than the H_3^+ ions emerging from the ion source, yet the branching ratio is noticeably higher from D_3. This result is a little surprising if it represents a real effect. It could result from a higher proportion of vibrational, compared to rotational energy, in the D_3^*, since vibrational excitation is more likely to yield complete dissociation.

The results from the hot discharge source gave average internal energies of 2.42 ± 0.2 eV for H_3 and 2.16 ± 0.2 eV for D_3, and 3-body/2-body ratios of 0.65 ± 0.06 and 0.57 ± 0.06, respectively. In this case the H_3^+ ions were apparently somewhat hotter than the D_3^+ ions. The rovibrational energies are approximately 1 eV less than the total internal energies (above the H + H + H asymptotic limit cited above). The measured average energies imply rovibrational energies of 1.4 and 1.2 eV for H_3^* and D_3^*, respectively. Except for the order, they are in rough agreement with the statistical calculations of Anicich and Futrell,[20] which predicted average vibrational energies of 1.3 and 1.5 eV, respectively, without considering angular momentum effects. The

different ordering of our results is notable but may be insignificant. Since the ions are formed in the reaction

$$H_2^+ + H_2 \rightarrow H_3^+ + H, \qquad (7)$$

which is 1.83 eV exothermic, and the initial H_2^+ reactants are formed vibrationally excited (averaging 0.8 eV[11]) by electron impact, the initial H_3^+ ions are expected to be formed both rotationally and vibrationally excited. The distributions that emerge from the ion source depend on the gas pressures and the residence times that allow relaxation.

The rovibrational energies depend primarily on the pressures and residence times in the ion sources, which were only approximately similar in each source. The one clear result here is that the 3-body/2-body branching ratio increases strongly with the internal energy in the predissociating Rydberg molecules. This result is not surprising, and is predicted in the calculations of Orel and Kulander,[20] but these are the first experimental data to show the energy dependence.

Also shown in Figure 7 are the theoretical results of Orel and Kulander.[19] Their time-dependent wave-packet studies of H_3 2s $^2A_1'$ predissociation were carried out in a two-dimensional approximation, which considered the symmetric and bending modes in C_{2v} symmetry, with no rotation. We have plotted the R_3/R_2 ratios from their Table I against the total energy minus the 4.48 eV dissociation energy of H_2, to compare with our results. The energy dependence is similar, but our ratios are lower, probably in part because our total energy is likely to contain a considerable amount of rotation, resulting from the ion-molecule Reaction (7), and the 3-body channel is probably inhibited by a rotational barrier.

Also shown in Figure 7 are ratios obtained by Mitchell et al.,[8,9] for the 3-body/2-body product branching of the dissociative recombination of H_3^+ for near-zero electron energies. This reaction is primarily a predissociation reaction involving very high Rydberg states near the

ionization limit, thus most of the internal energy is electronic. They used two ion sources: an r.f. discharge source, which produced hot ions, and an r.f. trap ion source, which produced ions primarily in v = 0. We have given the discharge source data the same rovibrational energy deduced in our Colutron source data, and have set their "cold" ion rovibrational energy at 0.07 eV. Note that H_3^+ (v = 0) is 4.75 eV above the H + H + H limit. A comparison of the branching ratios from dissociative recombination data with those resulting from predissociation of the n = 2 Rydbergs is interesting, indicating that the 3-body/2-body ratio is a steadily increasing function of total internal energy above the 3-body limit, and does not depend much on whether the energy is electronic or vibrational.

Comparison of our data to the theory of Orel and Kulander, which did not include rotational effects, may indicate that energy stored in rotation is not very effective in yielding 3-body products, compared to energy in vibrational modes. Perhaps this effect can be understood in a scenario where one atom leaves the complex relatively rapidly, and the remaining pair are inhibited from dissociating because of the rotational barrier.

B. Isotope effects.

As discussed above, we found very little difference between H_3 and D_3 in the 3-body/ 2-body branching ratios that wasn't easily attributable to different internal energies from their production in the Colutron source, however when it came to the preferred ejection of H or D from HD_2, the results were quite different.

We performed only a few experiments on the mixed isotopomers of H_3, and primarily on HD_2, because H_2D is indistinguishable from D_2 in our low resolution apparatus. Using an HD_2^+ ion beam produced by the hot discharge source, we measured the laboratory energies of both D and H atoms ejected from HD_2^*, corresponding to the reactions

$$HD_2^* \rightarrow D + HD, \text{ or} \qquad (8a)$$

$$HD_2^* \rightarrow H + D_2. \qquad (8b)$$

The two transformed spectra are shown in Figure 8, along with approximate deconvolutions. The difference between the D-atom spectrum, seen in Figure 8a, and the H-atom spectrum, in Figure 8b, is fairly dramatic. These first deconvolutions are fairly rough, but because in this asymmetric molecule we cannot make a reliable estimate of the 3-body energy scale to establish the internal energy, we did not attempt further refinements in the deconvolutions. We are primarily interested in the relative areas, which don't depend strongly on details of the deconvolutions. After normalizing the D/HD_2 spectrum so that 1/2 of it's 3-body area was equal to the area the 3-body spectrum in H/HD_2 (thus equating the total 3-body events in each), we found that among the 2-body products, the H atom has 2.7 ± 0.4 times the probability of each D atom to emerge, on a per atom basis.

The higher probability for the H atom ejection results from a faster predissociation rate for the H atom. Since the non-adiabatic elecronic coupling between the bound and continuum states is the same for both H and D, the faster rate for H results from better differential Franck-Condon factors, which are also direct factors in radially-coupled predissociation rates.[21] These factors will generally favor the H atom when the coupling occurs at close internuclear separations near the inner turning points of the bound and continuum states, as was recently found very strongly in NeH and NeD.[22]

On the other hand, when both H and D spectra from HD_2 are summed, the 3-body/2-body branching ratio was found to be 0.59 ± 0.1, which is very similar to the ratios obtained for both D_3 (0.58 ± 0.1) and H_3 (0.68 ± 0.1) using the same hot discharge source. Thus the H atom is preferred at the expense of the D atoms in the 2-body case, but the 3-body/2-body ratio is unchanged.

SUMMARY

We have made the first determinations of the 3-body/2-body product branching in the predissociation of the n = 2 Rydberg states of H_3. The ratio is found to increase steadily with the internal energy in the molecules. The data are consistent with higher ratios obtained from the dissociative recombination of H_3^+, when plotted against the total internal energy above the H + H + H limit, perhaps indicative of a similar predissociation channel. The data show a similar energy dependence as ratios obtained from a two-dimensional calculation by Orel and Kulander,[19] but are smaller in magnitude. Since the theory did not include the effects of rotational excitation, and our H_3* states are undoubtedly rotationally excited, our lower ratios may indicate that 3-body predissociation is inhibited by rotation.

Results from a brief examination of the HD_2 isotope show that the H atom has 2.7 ± 0.4 times the D probability, per atom, of being ejected in the 2-body case, indicating that the H atom predissociation rate is higher, as in other cases of predissociation by radial coupling of the electonic wave functions that occurs near the nuclear inner turning points.

ACKNOWLEDGEMENTS

We gratefully acknowledge support by the National Science Foundation under Grant PHY-8713309 and by the Air Force Office of Scientific Research under Contract No. F-49620-89-K-0002. CFH was supported by a grant from the Deutsche Forschungsgemeinschaft. WGG was on sabbatical leave from Queens University, Belfast, NI. We have benefitted greatly from interactions and conversations with A. Orel, K. Kulander, and our colleagues H. Helm, P. Cosby, and D. Huestis.

REFERENCES

1. G. Herzberg, *Ann. Rev. Phys. Chem.* **38**, 27 (1987).
2. I. Dabrowski and G. Herzberg, *Can. J. Phys.* **58**, 1238 (1980).
3. G. I. Gellene and R. F. Porter, *J. Chem. Phys.* **79**, 5975 (1983).
4. H. Helm, *Phys. Rev. Lett.* **56**, 42 (1986).
5. M. C. Bordas, P. C. Cosby, and H. Helm, *J. Chem. Phys.* **93**, (1990).
6. J. R. Peterson and Y. K. Bae, *Phys. Rev. A.* **30**, 2807 (1984).
7. P. C. Cosby and H. Helm, *Phys. Rev. Lett.* **61**, 298 (1988).
8. J.B.A. Mitchell, J. L. Forand, C. T. Ng, D. P. Levac, R. E. Mitchell, D. W. Mul, W. Claeys, A. Sen, and J. Wm. McGowan, *Phys. Rev. Lett.* **51**, 885 (1983).
9. H. Hus, F. Youssif, A. Sen, and J.B.A. Mitchell, *Phys. Rev. A* **38**, 658 (1988).
10. Y. K. Bae, M. J. Coggiola, and J. R. Peterson, *Phys. Rev. A* **31**, 3627 (1985).
11. D. P. de Bruijn, J. N. Neuteboom, and J. Los, *Chem. Phys.* **85**, 233 (1984).
12. H. Figger, M. N. Dixit, R. Maier, W. Schrepp, H. Walther, I. R. Peterkin, and J.K.G. Watson, *Phys. Rev. Lett.* **52**, 906 (1984); H. Figger, Y. Fukuda, W. Ketterle, and H. Walter, *Can. J. Phys.* **62**, 1274 (1984).
13. J. R. Peterson and Y. K. Bae, *Phys. Rev. A.* **34**, 3517 (1986).
14. C. Cisneros, I. Alvarez, C. F. Barnett, and J. A. Ray, *Phys. Rev. A.*, 76 (1976).
15. M. J. Coggiola, J. R. Peterson, and D. L. Huestis, *Phys. Rev. A.* **36**, 2008 (1987).
16. H. Helm, *Phys. Rev. A.* **38**, 3425 (1988).
17. K. Miethe, T. Dreiseidler, and E. Salzborn, *J. Phys. B* **15**, 3069 (1982).

18. D. K. Gibson and J. Los, *Physica* **35**, 258 (1967); M. Vogler and W. Seibt, *Z. Phys.* **210**, 337 (1968); T. T. Wornock and R. B. Bernstein, *J. Chem. Phys.* **49**, 1878 (1968).

19. A. E. Orel and K. C. Kulander, *J. Chem. Phys.* **91**, 6086 (1989).

20. V. G. Anicich and J. H. Futrell, *Int. J. Mass. Spect. Ion Proc.* **55**, 189 (1984).

21. A. L. Roche and J. Tellinghuisen, *Mol. Phys.* **38**, 129 (1979).

22. P. Devynck, W. G. Graham, and J. R. Peterson, *J. Chem. Phys.* **91**, 6880 (1989).

FIGURE CAPTIONS

Figure 1. Schematic potential energy diagram of H_3 and H_3^+. The arrow indicates the electron capture transition. Source: The absolute energies are taken from P. Cosby and H. Helm, Chem. Phys. Lett. **152**, 71 (1988).

Figure 2. Diagram of the apparatus, excluding the ion source and magnetic mass analyzer.

Figure 3. Laboratory energy spectrum of H^- atoms formed at 0° from a 3.2 keV H_3^+ beam transiting Cs vapor.

Figure 4. Transformed data from Figure 3. Solid line links 0° c.m. data; dots are 180° c.m. data.

Figure 5. Deconvoluted distributions from Fig. 4; energy scale is for the 2-body case. The initial H_3^+ ions were from the cooled hollow cathode source.

Figure 6. Deconvoluted H^- data from H_3^+ produced in the hot discharge source.

Figure 7. 3-body/2-body branching results from this experiment, compared to theory (Ref. 19) and to experimental results from dissociative recombination (Refs. 8 and 9).

Figure 8. Deconvoluted c.m. spectra of D^- and H^- data from HD_2 produced in the hot discharge source. Energy scale is for the two-body case in each of (a) and (b). See text.

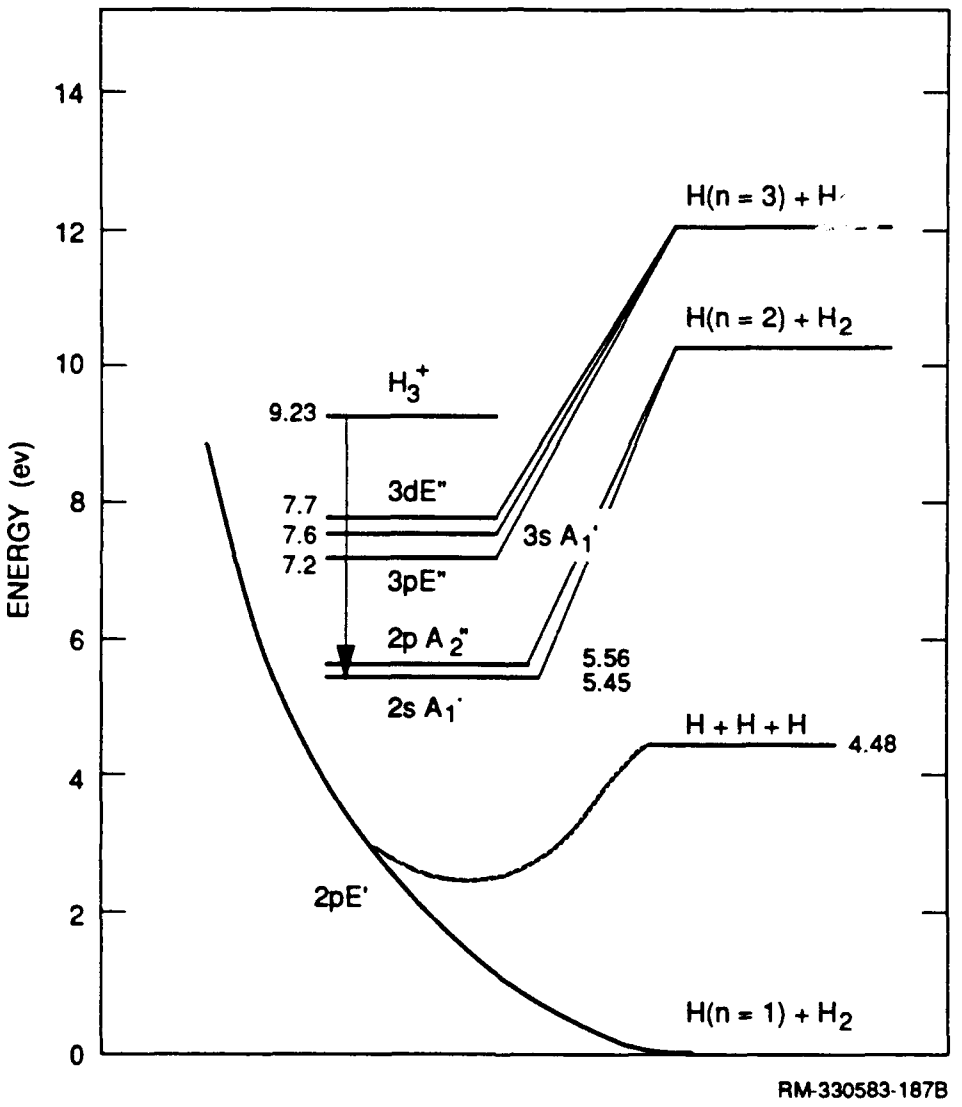
ENERGY (ev)
14
12
10
8
6
4
2
0
H(n = 3) + H
H(n = 2) + H2
H3+
9.23
3dE"
7.7
7.6
7.2
3pE"
3s A1'
2p A2"
5.56
5.45
2s A1'
H + H + H
4.48
2pE'
H(n = 1) + H2
RM-330583-187B

FIGURE 1

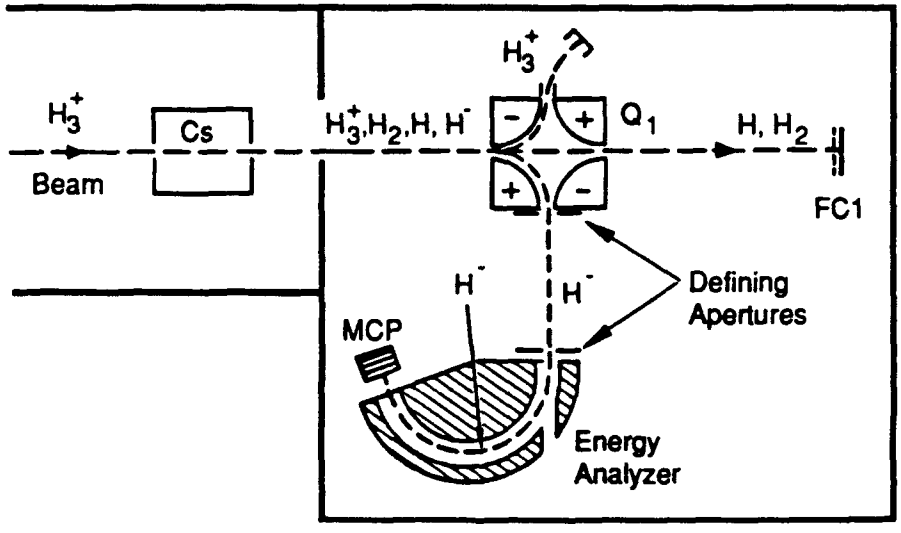
H_3^+
Cs
Beam
H_3^+
H_3^+, H_2, H, H^-
Q_1
H, H_2
FC1
H^-
H^-
Defining Apertures
MCP
Energy Analyzer
JM-1269-35F

FIGURE 2

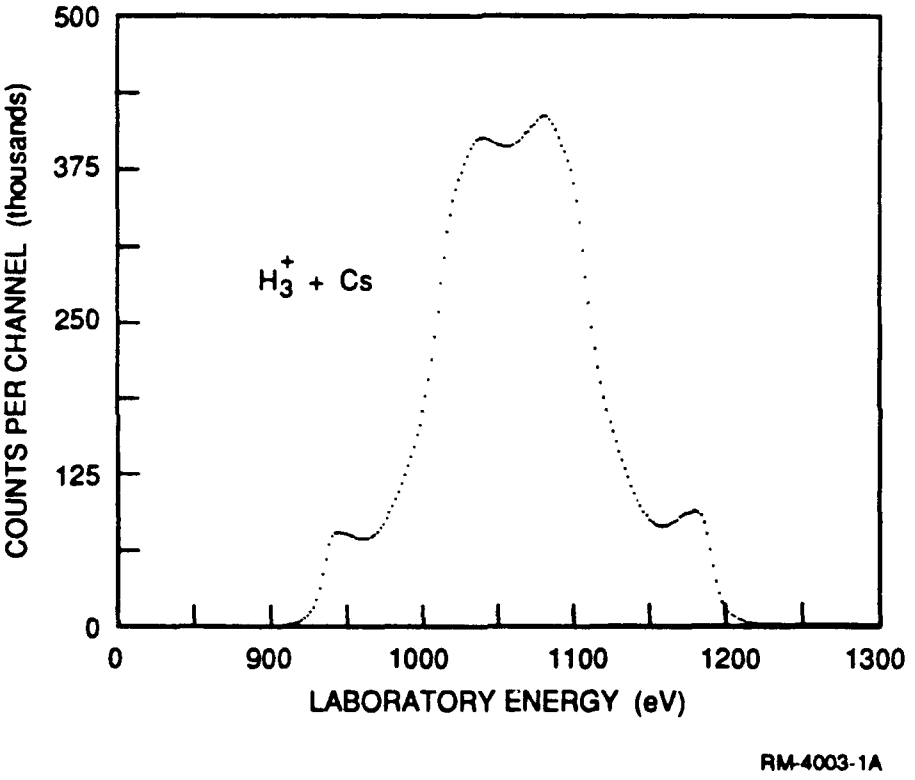
500
375
250
125
0
COUNTS PER CHANNEL (thousands)
H_3^+ + Cs
0
900
1000
1100
1200
1300
LABORATORY ENERGY (eV)
RM-4003-1A

FIGURE 3

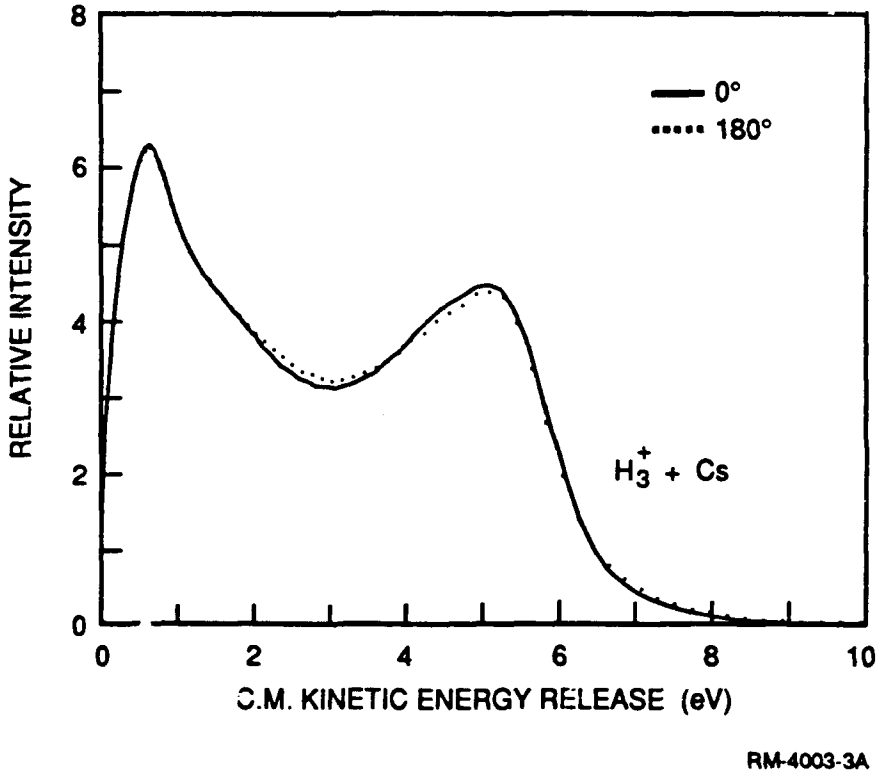
8
6
4
2
0
0
2
4
6
8
10
RELATIVE INTENSITY
C.M. KINETIC ENERGY RELEASE (eV)
0°
180°
H_3^+ + Cs
RM-4003-3A

FIGURE 4

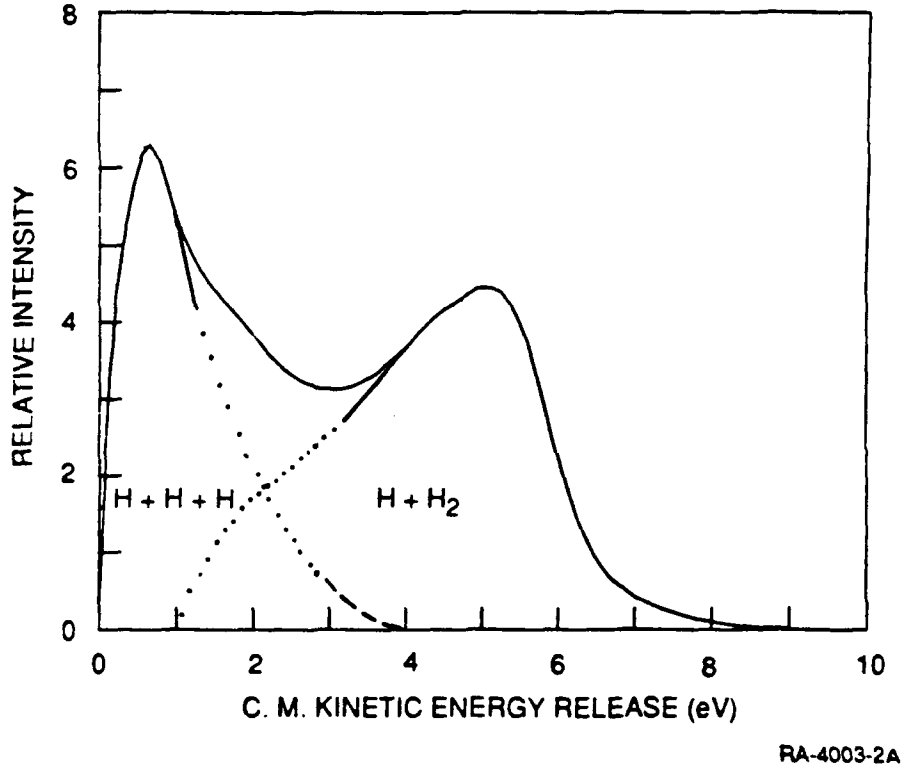
8
6
4
2
0
RELATIVE INTENSITY
H + H + H
H + H2
0
2
4
6
8
10
C. M. KINETIC ENERGY RELEASE (eV)
RA-4003-2A

FIGURE 5

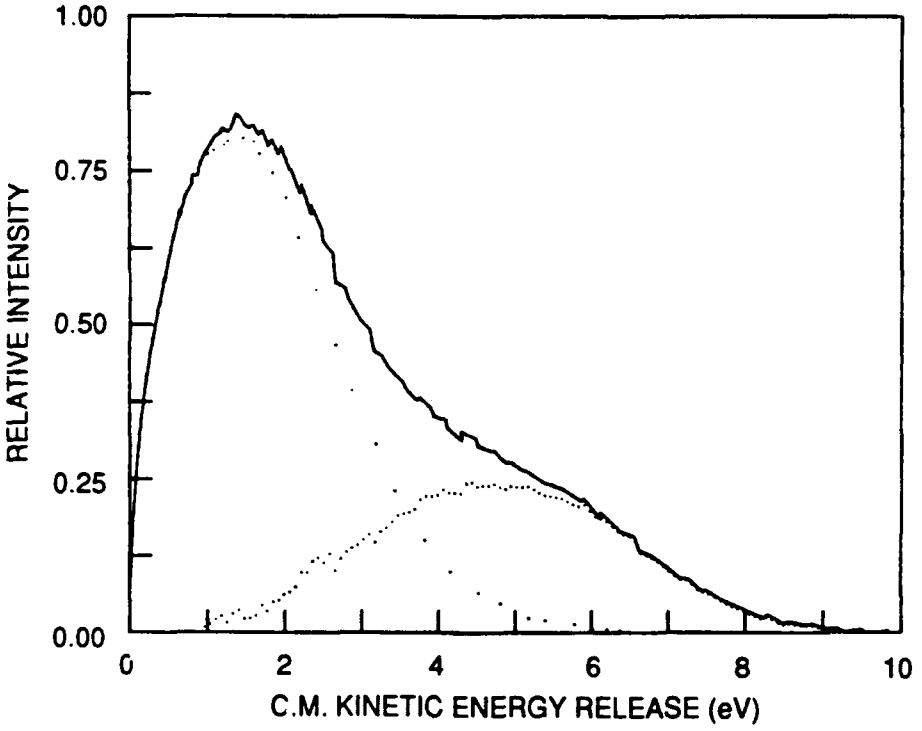
1.00
0.75
0.50
0.25
0.00
RELATIVE INTENSITY
0
2
4
6
8
10
C.M. KINETIC ENERGY RELEASE (eV)
RM-6952-47

FIGURE 6

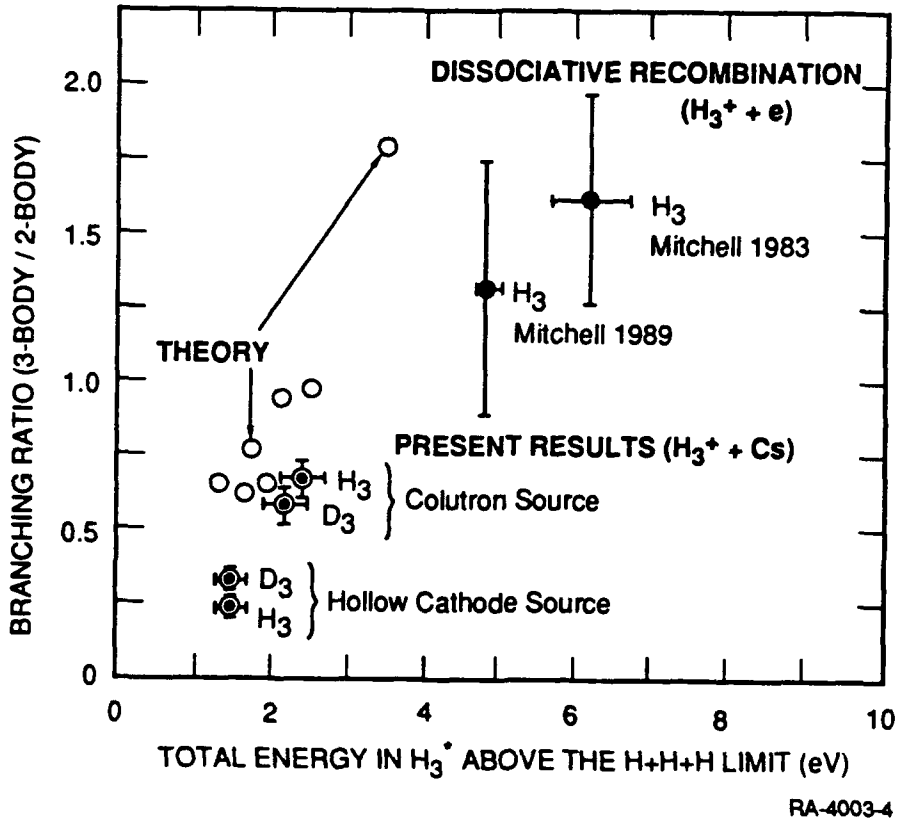
DISSOCIATIVE RECOMBINATION
(H_3^+ + e)
H_3
Mitchell 1983
H_3
Mitchell 1989
THEORY
PRESENT RESULTS (H_3^+ + Cs)
H_3
D_3
Colutron Source
D_3
H_3
Hollow Cathode Source
BRANCHING RATIO (3-BODY / 2-BODY)
2.0
1.5
1.0
0.5
0
0
2
4
6
8
10
TOTAL ENERGY IN H_3^* ABOVE THE H+H+H LIMIT (eV)
RA-4003-4

FIGURE 7

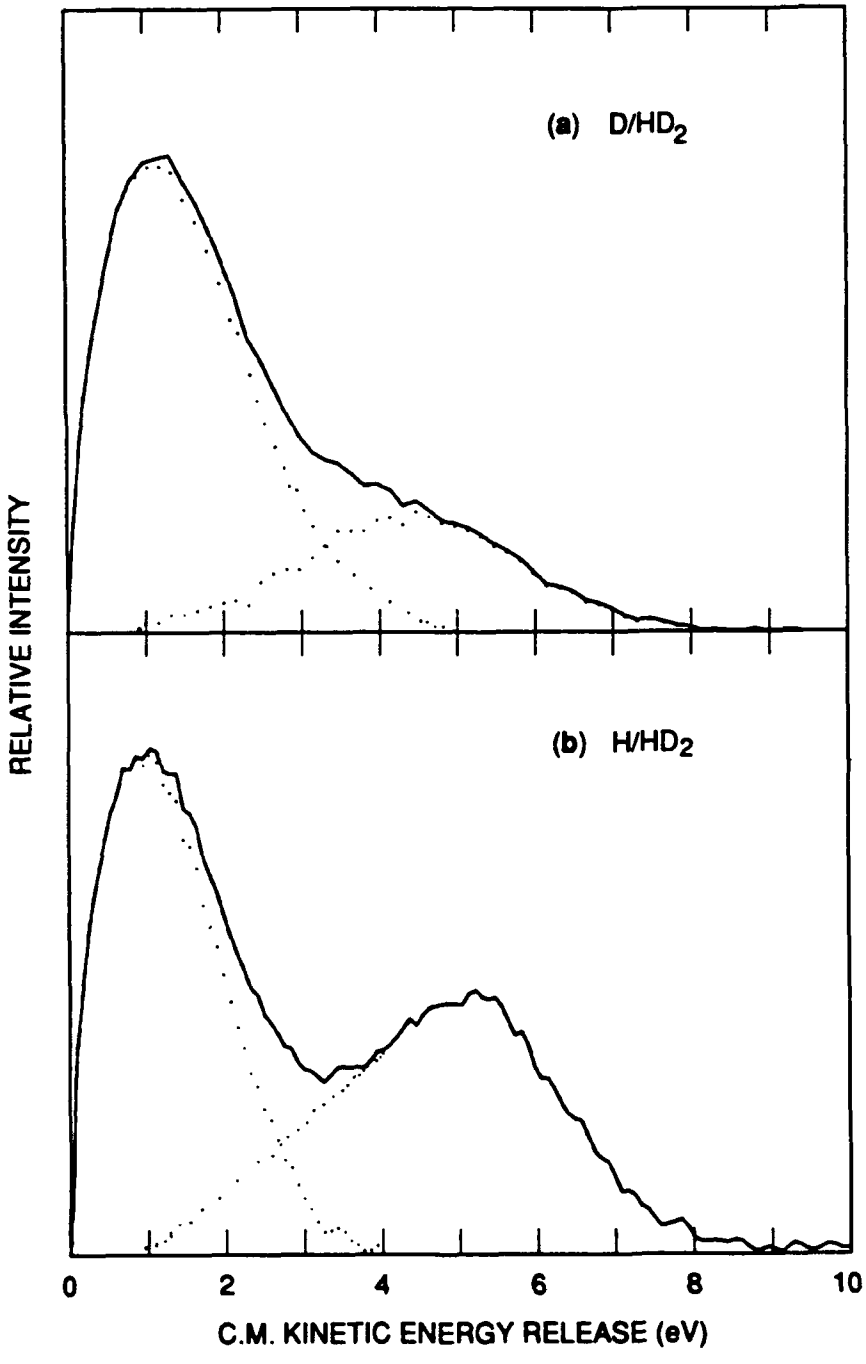
(a) D/HD2
(b) H/HD2
RELATIVE INTENSITY
0
2
4
6
8
10
C.M. KINETIC ENERGY RELEASE (eV)
RAM-6952-48

FIGURE 8

Appendix B

A SHAPE RESONANCE IN Ca^- PHOTODETACHMENT AND THE ELECTRON AFFINITY OF Ca (^1S)

A SHAPE RESONANCE IN Ca^- PHOTODETACHMENT AND THE ELECTRON AFFINITY OF Ca (^1S)

C. W. Walter and J. R. Peterson
Molecular Physics Laboratory
SRI International
Menlo Park, CA 94025

ABSTRACT

It was only recently found that a stable negative ion Ca^- ^2P exists below the Ca (^1S) ground state. An electron affinity of 43 ± 7 meV was obtained experimentally, and numerous theoretical calculations have now found values between 0 and 100 meV. We report the first photodetachment threshold measurements on Ca^-, which display a p-wave threshold above Ca $4s4p\,^3P$ and a large p-wave shape resonance above Ca $4s4p\,^1P$. Both threshold energies obtained from the data agree with a new electron affinity of 18.4 ± 2.5 meV for Ca (^1S).

MP 91-248
December 2, 1991

Among the many testing grounds for *ab initio* calculations of atomic energy levels, Ca^- is proving to be among the most challenging. Prior to 1987 the ^1S ground states of alkaline-earth atoms, with closed ns^2 subshells, were predicted theoretically to have negative electron affinities, analogous to the rare gases. Then, Froese Fischer et al.[1] found theoretically that Ca^- exists stably in a $4s^24p\ ^2P$ state, bound by about 45 meV below Ca (^1S), in agreement with measurements of Pegg et al.,[2] who had earlier found evidence of a stable Ca^- state and subsequently measured an electron affinity EA(^1S) of 43 ± 7 meV.[2] In the following four years at least ten other calculations[3-12] have examined alkaline earth negative ions, with most finding Ca EA's in the 40-80 meV range, but with no consistent agreement. Calculations of higher accuracy are extremely difficult because, as Bates[13] points out, 40 meV is only 2×10^{-6} of the total electronic energy in Ca. Until now, there have been no other experimental determinations.

In another vein, the first results on stable Ca^- [1,2] led Johnston et al.[14] to reexamine their earlier data on electron transmission through Ca vapor. The energy-differential currents revealed two dominant features, a broad resonance at 1.1 ± 0.15 eV and a sharp resonance at 2.8 ± 0.15 eV. The data were also compared with early low-resolution Ca^- photodetachment measurements by Heinicke et al.[15], which showed structures at similar energies: a broad minimum near 1 eV and a narrow maximum near 2.9 eV. It is now clear that the Ca^- beam in the experiments of Heinicke et al.,[15] which was extracted directly from an ion source, was predominantly in the stable ^2P state; however, because of the existing belief that Ca^- was unstable, they had considered the ions to be in long-lived (> 10 μs) excited states of ^4F or ^4P configuration. In fact, a metastable $4s4p^2\ ^4P$ state was eventually predicted theoretically by Bunge et al.[16] to be quite strongly bound by 550 meV below Ca ^3P. These calculations on $Ca^-\ ^4P$ were first substantiated by work in our laboratory, in which we determined the EA(^3P) = 562 ± 15 meV and measured a decay lifetime of 0.29 ± 0.10 ms.[17] In an extension of the work on ^4P, we recently sought evidence of the ^2P state of Ca^- in our beam, by photodetachment near the $^2P \rightarrow 4s4p^3P + kp$ threshold, expected near hν = 1.93 eV. We indeed found a p-wave threshold,[18] but its location near 1.90 eV placed the

EA(^{1}S) closer to 15 meV than the 43 meV of Pegg et al.[2] We again observed the p-wave threshold near 2.6 eV that we had attributed earlier to the ^{4}P state,[17] but now we were concerned that this structure might instead be connected with the doublet resonance near 2.8 eV discussed by Johnston et al.[14] It became clear that more measurements were needed at higher photon energies near 2.8 eV.

We report here on new photodetachment measurements in the region 2.8-3.1 eV. The data reveal a large p-wave shape resonance located near 3 eV. Analysis of this structure both characterizes the resonance and establishes the energy of the Ca (^{1}P) threshold, from which we derive a new electron affinity of 18.4 ± 2.5 meV for ground state Ca (^{1}S).

Except for minor modifications, the experimental setup has been described before.[17] Ca^+ ions were extracted from a Colutron ion source, accelerated to 3 keV, focused, magnetically mass-analyzed, and directed through a Cs-vapor charge transfer cell and into a separately pumped interaction chamber (pressure ~ 3×10^{-7} Torr). The beam then entered an electrostatic quadrupole Q1 which separated the various charge states exiting the charge transfer cell (Ca^+, Ca^0, Ca^-) and deflected the Ca^- ions 90°, onto an 8 cm drift path and into a second quadrupole Q2, which directed them into a current monitor. Between the two quadrupoles, the ion beam was merged coaxially with a laser beam from an Ar^+ laser-pumped cw dye laser (linewidth ~0.5 Å). Neutral Ca atoms formed along the Q1-Q2 drift path passed through Q2 and struck the front surface of a quartz plate coated with a thin (~40 Å) film of gold, from which secondary electrons were ejected and accelerated to a channeltron electron multiplier, whose output pulses were amplified and counted. The laser beam then passed through the coated quartz plate (about 40% was absorbed or reflected) and was monitored after it exited the vacuum.

Fast Ca neutrals could be formed along the Q1-Q2 drift path from Ca^- either by photo- or autodetachment, or by collisions with the background gas. The photon dependent component was determined by mechanically chopping the laser beam, and using a CAMAC-based gated two-channel counter to provide the on-off difference and sums of the channeltron output. The laser

was then scanned under computer-control and the photodetachment signal recorded as a function of laser frequency. At the higher photon energies above 2.8 eV, there was an additional laser-produced signal resulting from photoelectrons ejected from the gold surface of the quartz plate. This additional signal was evaluated by scanning the laser with the ion beam off, before and after each photodetachment scan, and subsequently subtracted from the data. The relative photodetachment cross sections were determined by normalizing the measured detachment signal to the transmitted laser power and the negative ion beam current. In order to obtain a consistent laser-ion beam overlap for each measurement, the laser beam position was centered on two apertures placed external to the vacuum chamber at the entrance and exit windows. Using this procedure, the relative cross sections showed satisfactory internal consistency over a wide range of photon energies obtained with several different dyes used in the tunable laser.

We have now used, in addition to the dye laser, a tunable cw Ti:Sapphire laser to cover almost continuously an extensive photon energy range from 1.13 to 3.04 eV. Most of the data are shown in Figure 1; the complete results will be published separately. We concentrate here on the narrow region 2.9-3.04 eV, for which Stilbene 1 dye was used in the dye laser.

We draw attention to the cross section near the ^1P threshold in Figure 1. A large sharp peak in the cross section occurs near 3.0 eV on top of a slowly increasing background resulting from detachment to lower energy continua, including the $^4P \rightarrow {}^3S + kp$ channel studied earlier.[17] The data in this region are shown in greater detail in Figure 2. The peak has the characteristic form of an electronic shape resonance, similar to the $He^-(1s2p^2\ ^4P)$ shape resonance that was well resolved in our earlier work in He^- photodetachment.[19] In shape resonances, the ejected electron is temporarily bound inside the centrifugal potential barrier created by its own orbital angular momentum $\ell > 0$. A shape resonance is located above its parent neutral state, and it decays primarily into that continuum, thus it gives only a positive contribution to the total cross section, and will appear asymmetrical if close to threshold. In contrast, Feshbach states lie below the parent neutral state and decay by configuration interaction with the continuum of one or more

lower neutral states. Thus they decay slower and are narrower than shape types, and also exhibit destructive as well as constructive interference with the underlying continua, as described by Fano.[20]

The 3.0 eV peak has the asymmetric, non-interference structure of a shape resonance, and its energy suggests a p-wave shape resonance above the $4s^24p\ ^2P \rightarrow 4s4p\ ^1P + kp$ threshold $E_0(^1P)$, which is 2.93 eV above $Ca(^1S)$. this interpretation is justified by the following data analysis, whose goal is to determine $E_0(^1P)$ and thus $EA(^1S)$.

In the absence of resonances or interactions with lower continua, the photodetachment cross section just above an opening channel with continuum electron of angular momentum ℓ and linear momentum k follows the Wigner threshold law $\sigma \sim k^{2\ell+1}$. However, as observed in He^- by Peterson, Bae, and Huestis,[19] the Wigner law fails quickly above the threshold because of the strong influence of the resonance. They derived a modified threshold formula specifically to include the effects of a p-wave shape resonance.[19] An approximate form, their Eq. 10, can be expressed as

$$\sigma(E) \sim (E-E_0)^{3/2}\,[(E-E_R)^2 + (\Gamma/2)^2]^{-1} \qquad (1)$$

where E is the photon energy, E_0 is the threshold of the opening state, E_R is the resonance energy, and $\Gamma/2$ is the half width of the resonance (inverse lifetime/$\hbar$). It can be seen that this approximate form is simply a Wigner threshold numerator with a dispersion-type resonance denominator. Although derived specifically to describe near-threshold data, this formula can give a reasonable fit to the entire resonance.[19]

In order to apply Eq. (2), the various fine-structure transitions between initial and final states must be considered. Here the initial Ca^- state is a doublet consisting of $^2P_{1/2}$, the ground state, and $^2P_{3/2}$, separated by the fine-structure interval ΔE_{fs}. The final state of Ca is a singlet, $Ca(^1P)$. We neglect any fine-structure splitting in the $Ca^-(^2D)$ resonance; it is probably small and its effect on the determination of E_o is negligible. Equation (2) can then be rewritten

$$\sigma(E) = \sigma_o + AE + B\left\{\frac{(E-E_0)^{3/2}}{(E-E_R)^2 + (\Gamma/2)^2} + \frac{W\ [E-(E_0 - \Delta E_{fs})]^{3/2}}{[E-(E_R - \Delta E_{fs})]^2 + (\Gamma/2)^2}\right\} \qquad (2)$$

where E_0 and E_R are relative to the $Ca^-(^2P_{1/2})$ ground state, W is the population of J = 3/2 relative to that of J = 1/2, and B is a normalization constant. The background continuum contribution to the photodetachment cross section is approximated by the constant σ_0 plus a linearly energy-dependent term of slope A (determined from the cross section below threshold and assumed to be constant over the peak). ΔE_{fs} in $Ca^-(^2P)$ has been calculated by Dzuba et al,[21] who report ΔE_{fs} = 6.9 meV, and by Brage and Froese Fischer,[22] who obtain 4.2 meV. In contrast to the considerable uncertainty in calculations of the absolute electron affinity, the fine-structure interval calculations should be much more reliable because the correlation contributions (difficult to calculate) are nearly identical for the $^2P_{1/2}$ and $^2P_{3/2}$ state energies. In the analysis that follows, we take ΔE_{fs} = 5.6 meV, the average of these values. The relative populations of the fine-structure levels are assumed to be given by the statistical weights of the initial J = 1/2 and 3/2 states, i.e., W = 2. This assumption seems reasonable because of the small energy separation.

The resonance parameters in Eq. (3) were established by a least squares fit to all the data within 100 meV of the threshold. This fit, shown as the solid line in Fig. (2), gave E_R = 2.9673 eV and $\Gamma/2$ = 0.0173 eV. Next, the resonance parameters were fixed at these values and the higher resolution data within only 15 meV of threshold were fit to yield E_0 = 2.9509 eV, which represents the threshold for the $Ca^-(^2P_{1/2}) \rightarrow Ca(^1P) + kp$ transition. The modified threshold formula of Eq. (3) provides a satisfactory fit to the entire resonance, and a very good fit to the threshold data, as seen in Figure 3. Extension of the measurements to higher photon energies was prevented by our inability to operate the dye laser at shorter wavelengths.

The fit to all the data fixes E_R at 16.3 meV above E_0, and $\Gamma/2$ = 17.3 meV. Such nearly equal magnitudes of $\Gamma/2$ and E_R-E_0 were also observed in the $^4P^e$ shape resonance in He^-,[19] and

this characteristic probably typifies shape resonances in general.[14,19] The similarity here supports our interpretation of the resonance as associated with (located above) the ^1P state instead of the ^3P state, as suggested by Johnston et al.[14] If the parent state of the shape resonance were the lower ^3P state at 1.89 eV, the halfwidth would be much broader than 17 meV.

From the measured threshold energy $E_0(^1P)$ we can determine the binding energy of $Ca^-(^2P)$, i.e., $EA(^1S)$, via the relation

$$EA(^1S) = E_0(^1P) - E(^1P), \tag{3}$$

where $E(^1P) = 2.9325$ eV is the spectroscopically established energy of the Ca ^1P state relative to ^1S. Using $E_0 = 2.9509$ eV, we obtain $EA(^1S) = 18.4 \pm 2.5$ meV. This value is the binding energy of the $Ca^-(4s^24p^2P_{1/2})$ ground state. The uncertainty results primarily from determining the slope and magnitude of the continuum and from the uncertainty in ΔE_{fs} (the fit itself yields an uncertainty ~1.0 meV). This value of $EA(^1S)$ is in agreement with the less certain value of 15 ± 6 meV obtained from reanalysis of the lower ^3P threshold seen in Fig. 1, whose onset is much less distinct and more uncertain because of the fine-structure splittings in the Ca ^3P state. Thus data from two separate thresholds agree with the value $EA(^1S) = 18.4 \pm 2.5$ meV, in disagreement with the 43 ± 7 meV obtained by Pegg et al.[2] Although we have sought an explanation for the difference (in consultation with D. Pegg and R. Compton), we have found none as yet. However the agreement of our determination from the two separate thresholds establishes strong confidence in it.

The experimentally determined electron affinities are tabulated along with a summary of theoretically calculated values in Table I. The uncertainty in the various calculations is manifested in the lack of agreement among them and, as mentioned above, reflects the difficulty of obtaining an uncertainty of even 50 meV in the calculations when it is only $\sim 10^{-6}$ of the total energy. Nevertheless, such accuracy is a challenge to the calculations, and will doubtless be achieved when

all of the correlation, relativistic, and core polarization effects are adequately accounted for, along with the use of suitably large wave function basis sets.

In summary, we have determined a new value for the electron affinity of $Ca(^1S)$ using photodetachment threshold spectroscopy and characterized a large shape resonance in Ca^- located just above the $Ca(^1P)$ state. Our experimental method, which detects the fast neutral Ca atoms following photodetachment, has an important advantage over the detection of the detached electrons: the detection efficiency is independent of the kinetic energy of the electrons. The data represent the total photodetachment cross sections of the ions in the beam, thus the shapes of the structures in the cross sections have physical meaning and can be analyzed accordingly. The observed structures represent opening states or resonances that occur in the continua of lower thresholds, so that some care must be given to their interpretation. The energy of the ^2P negative ion, the location and width of the shape resonance, and the resultant photodetachment cross sections are important quantities that can, and should, be calculated in more detail for comparison with the present experimental results.

We thank Charlotte Froese Fischer and Tomas Brage, Paul Burrow and Gordon Gallup for very useful conversations and for sharing their results. We thank David Pegg and Robert Compton for useful discussions of their experiment, and Wilfried Meyer, Charles Bauschlicher and Peter Taylor for illuminating the capabilities and limitations of current theory. Locally we have benefitted greatly from discussions with David Huestis and Roberta Saxon. We gratefully acknowledge the support of the National Science Foundation under grants PHY 87-13309 and 91-11872, and the Air Force Office of Scientific Research under contract F49620-89-K-0002.

REFERENCES

1. C. Froese Fischer, J. B. Lagowski, and S. H. Vosko, Phys. Rev. Lett. **59**, 2263 (1987).

2. D. J. Pegg, J. S. Thompson, R. N. Compton, and G. D. Alton, Phys. Rev. Lett. **59**, 2267 (1987).

3. C. Froese Fischer, Phys. Rev. A **39**, 963 (1989).

4. S. H. Vosko, J. B. Lagowski, and I. L. Mayer, Phys. Rev. A **39**, 446 (1989).

5. L. Kim and C. H. Greene, J. Phys. B: At. Mol. Opt. Phys. **22**, L175 (1989).

6. C. W. Bauschlicher, S. R. Langhoff and P. R. Taylor, Chem. Phys. Lett. **158**, 245 (1989).

7. W. R. Johnson, J. Sapirstein, and S. A. Blundell, J. Phys. B: At. Mol. Opt. Phys. **22**, 2341 (1989).

8. G. F. Gribakin, B. V. Gul'tsev, V. K. Ivanov, and M. Yu Kuchiev, J. Phys. B: At. Mol. Opt. Phys. **23**, 4505 (1990).

9. C. W. Bauschlicher, S. R. Langhoff, and P. R. Taylor, Chem. Phys. Lett. **158**, 245 (1989).

10. P. Fuentealba, A. Savin, H. Stoll, and H. Preuss, Phys. Rev. A **41**, 1238 (1990).

11. R. D. Cowan and M. Wilson, Physica Scripta **43**, 244 (1991).

12. T. Brage and C. Froese Fischer, Proc. Conf. Comput. Quantum Phys., C. Bottcher, V. E. Oberacher, M. R. Strager, and A. S. Umar, Eds. (AIP, New York, 1991), in press.

13. D. R. Bates, Adv. Atomic Molec. Phys. **27**, 1 (1991).

14. A. R. Johnston, G. A. Gallup, and P. D. Burrow, Phys. Rev. A **40**, 4770 (1989).

15. E. Heinicke, H. J. Kaiser, R. Rackwitz, and D. Feldman, Phys. Lett. **50A**, 265 (1974).

16. C. F. Bunge, M. Galán, R. Jauregui, and A. V. Bunge, Nucl. Instrum. Methods Phys. Res. **202**, 299 (1982).

17. D. Hanstorp. P. Devynck, W. G. Graham, and J. R. Peterson, Phys. Rev. Lett. **63**, 368 (1989).

18. C. W. Walter, C. F. Hertzler, and J. R Peterson, Bull. Am. Phys. Soc. **36**, 1375 (1991).

19. J. R. Peterson, Y. K. Bae, and D. L. Huestis, Phys. Rev. Lett. **55**, 692 (1985).

20. U. Fano, Phys. Rev. **124**, 1866 (1961).

21. V. A. Dzuba, V. V. Flambaum, G. F. Gribakin, D. P. Sushkov, Phys. Rev. A. **44**, 2823 (1991).

22. T. Brage and C. Froese Fisher, unpublished (1991).

Table 1

ELECTRON AFFINITIES FOR Ca (^{1}S), IN meV

Reference	Method	EA
Experimental		
Present work (1991)	Photodet. Thresh.	18.4 ± 2.5
Pegg et al (1987)[2]	Photoelec. Spectr.	43 ± 7
Theoretical		
Valence Correlation Only		
Froese Fischer et al. (1987)[1]	MCHF	45
Froese Fischer (1989)[3]	MCHF	62
Kim and Greene (1989)[5]	R matrix	70
Gribakin et al. (1990)[8]	Dyson equation	58
Cowan and Wilson (1991)[11]	HFR	82
Core-Valence Correlation		
Johnson et al. (1989)[7]	Dyson equation	56
Bauschlicher et al. (1989)[9]	SOCI	22
Fuentealba et al. (1990)[10]	CI + CV	0
Brage and Fischer (1991)[12]	MCHF + CV	47

FIGURE CAPTIONS

Figure 1 Total photodetachment cross sections above 1.8 eV; arrows indicate various thresholds. Note the shape resonance near 2.9 eV.

Figure 2 Data in the region of the shape resonance, and a fit to them using the modified threshold law, Eq. (3), to obtain E_R and $\Gamma/2$.

Figure 3 Finely spaced data over a 30 meV range near the ^1P threshold, and a fit using Eq. (3) to obtain E_0. $E_0(1/2, 3/2)$ indicate the thresholds for $^2P_{1/2, 3/2} \rightarrow {}^1P + kp$.

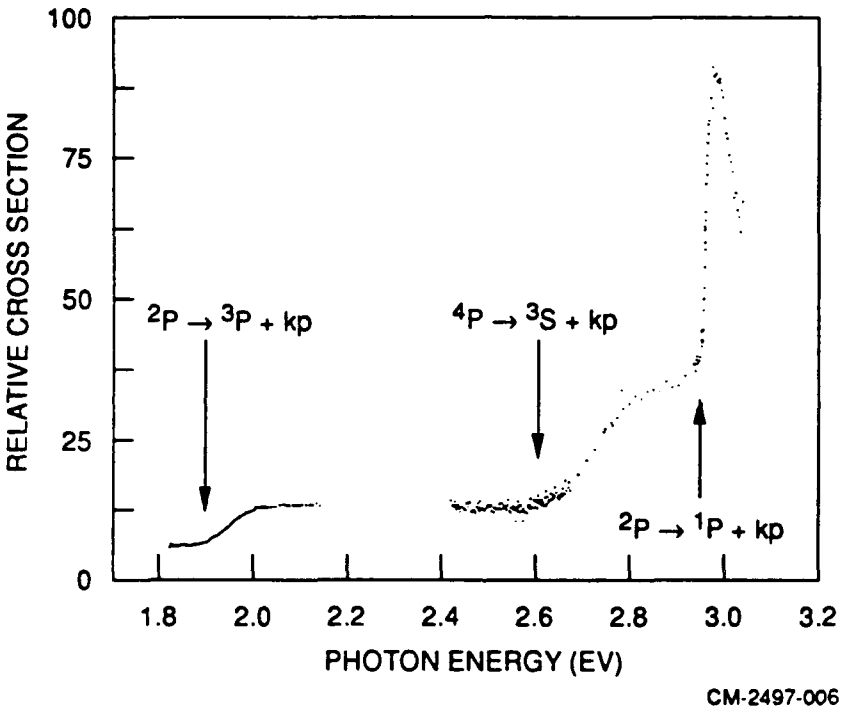
100
75
50
25
0
RELATIVE CROSS SECTION
$^2P \rightarrow {}^3P + kp$
$^4P \rightarrow {}^3S + kp$
$^2P \rightarrow {}^1P + kp$
1.8
2.0
2.2
2.4
2.6
2.8
3.0
3.2
PHOTON ENERGY (EV)
CM-2497-006

Figure 1

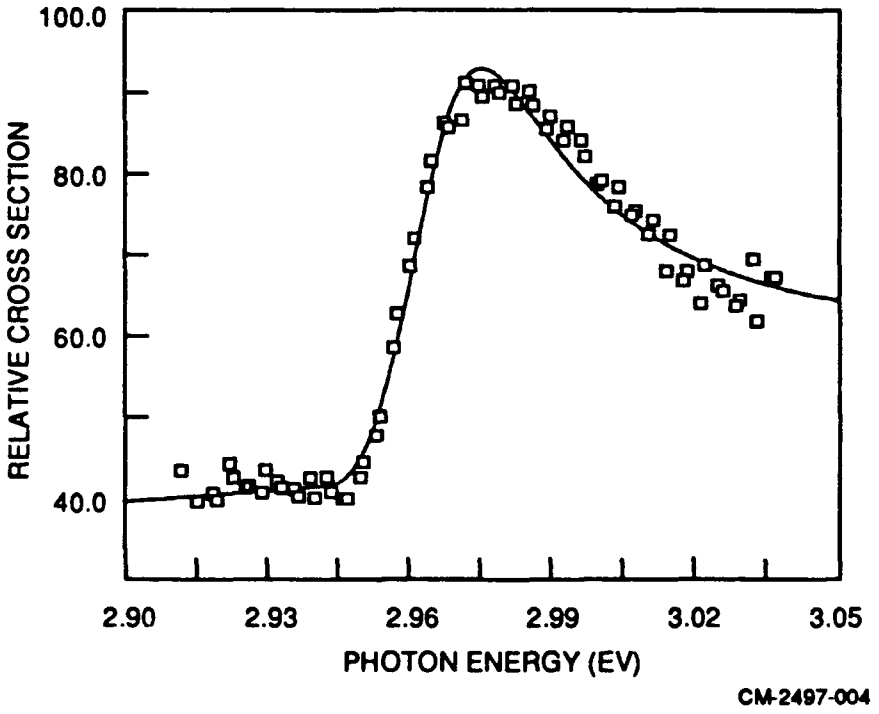
100.0
80.0
60.0
40.0
RELATIVE CROSS SECTION
2.90
2.93
2.96
2.99
3.02
3.05
PHOTON ENERGY (EV)
CM-2497-004

Figure 2

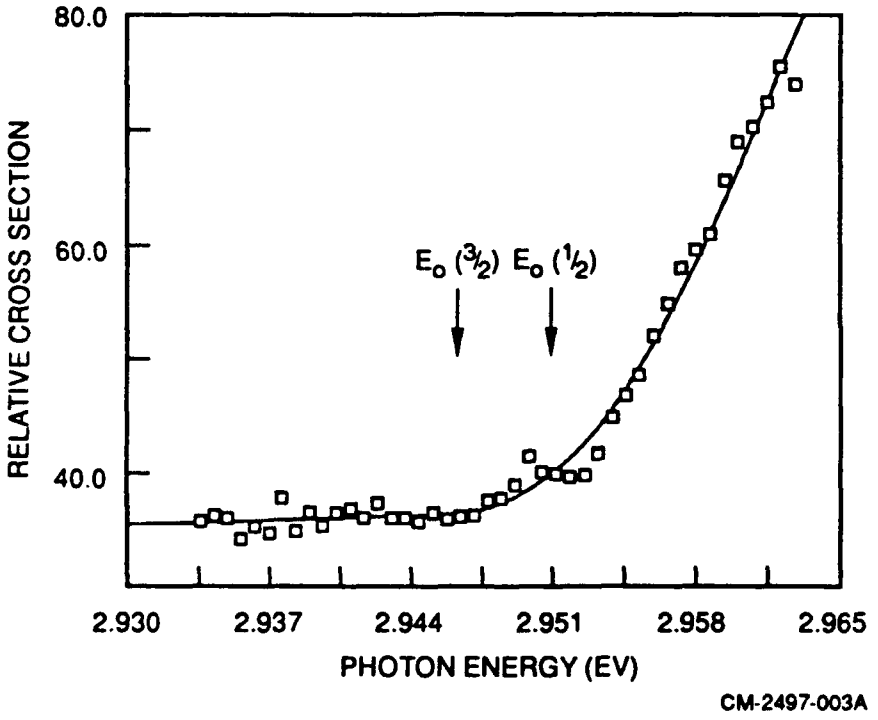
80.0
60.0
40.0
RELATIVE CROSS SECTION
E_o (3/2) E_o (1/2)
2.930
2.937
2.944
2.951
2.958
2.965
PHOTON ENERGY (EV)
CM-2497-003A

Figure 3

Appendix C

DETERMINATION OF RO-VIBRATIONAL PRODUCT DISTRIBUTIONS IN ION-MOLECULE REACTIONS

DETERMINATION OF RO-VIBRATIONAL PRODUCT DISTRIBUTIONS IN ION-MOLECULE REACTIONS

C. W. Walter, J. R. Peterson, and P. C. Cosby

Molecular Physics Laboratory
SRI International
Menlo Park, CA 94025 USA

Charge transfer neutralization of O_2^+ ($X^2\Pi_g$) in Cs vapor at keV energies has been found to preferentially populate the O_2 3sσ Rydberg states $d^1\Pi_g$ and $C^3\Pi_g$, which rapidly predissociate to neutral atoms.[1] Because the ionic core of the Rydbergs is essentially identical to that of $O_2^+(X)$ and the charge transfer cross sections are quite large (~100Å^2), the rovibrational population in the reactant ion is reproduced in the product Rydberg state, and finally appears in discrete translational energy releases to the dissociation fragment atoms. These fragment atom pairs are monitored by a position and time sensitive detector[2] which determines the center-of-mass fragment energy release spectrum and, thereby, serves as an extremely sensitive diagnostic of the reactant ion rovibrational population.

We have applied this technique to study the internal energy of O_2^+ produced in the reaction:

$$O^+ + CO_2 \rightarrow O_2^+(v=0\text{-}5) + CO, \qquad (1)$$

which is believed to occur in rocket exhaust plumes in the ionosphere. Reaction (1) is exothermic only for O_2^+ products in $v \leq 5$. The reaction was produced in a Nier-type electron-impact ion source filled with CO_2 gas (estimated pressure 0.2 - 1 Torr) and using a very small repeller voltage (< 1V). For comparison, O_2^+ ions were also produced in pure O_2 gas and in a 6% mixture of O_2 in N_2 at a variety of pressures under otherwise identical source conditions.

Comparison of the dissociative charge transfer product spectra for O_2^+ produced in O_2 (top) and CO_2 (bottom) is shown in Fig. 1. The doubling of the peaks, most apparent for v = 0,1, reflects the small energy separation of the $d^1\Pi_g$ and $C^3\Pi_g$ states, each predissociating to $O(^1D) + O(^3P)$. The width of individual vibrational peaks largely manifests the distribution of unresolved rotational levels. In the low pressure O_2 spectrum, the approximate rotational temperature is 550K and the vibrational populations reflect the Franck-Condon factors for ionization. Neither the rotational temperature nor the vibrational distribution change substantially when O_2^+ is produced from the O_2/N_2 mixture even at high pressure, but significant vibrational relaxation occurs in high pressure O_2, as expected for resonant charge-transfer.[3] Qualitatively, the O_2^+ produced in (1) is rotationally much hotter and has a unique vibrational distribution that, as expected, terminates at v = 5.

Quantitative rotational and vibrational distributions for reaction (1) will be presented and compared with a recent determination[4] in a selected-ion flow tube.

Research supported by NSF grant PHY-871330 and by AFOSR Contract F49620-89-K-0002.

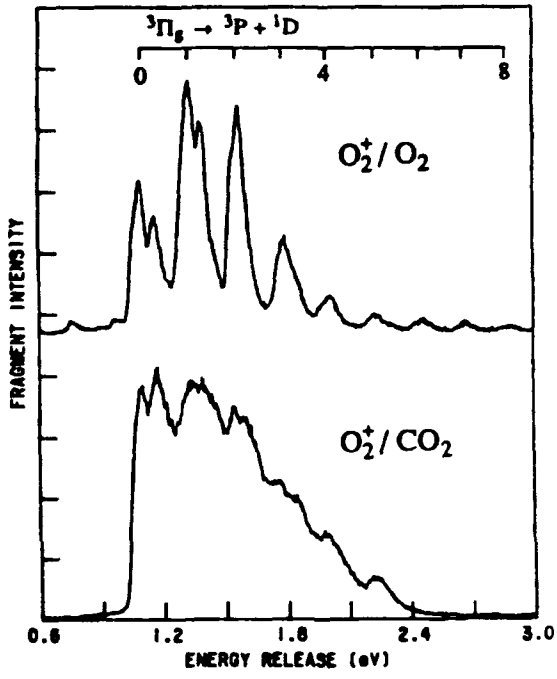

Figure 1. Dissociative charge transfer product translational energy release for $O_2^+(X^2\Pi_g)$ produced by electron impact (180 eV) in low pressure O_2 (top) and high pressure CO_2 (bottom). The energies of $C^3\Pi_g$ state vibrational levels are shown at the top of the figure.

References

1. W. J. Van Der Zande, W. Koot, J. R. Peterson, and J. Los, Chem. Phys. Lett. **140**, 175 (1987).

2. H. Helm and P. C. Cosby, J. Chem. Phys. **86**, 6813 (1987).

3. T. F. Moran, K. J. McCann, M. Cobb, R. F. Borkman, and M. R. Flannery, J. Chem. Phys. **74**, 2325 (1981).

4. A. A. Viggiano, R. A. Morris, F. Dale, and J. F. Paulson, J. Chem. Phys. **93**, 1681 (1990).